

This is the peer reviewed version of the following article:

Multiple Viral Ligands Naturally Presented by Different Class I Molecules in
Transporter Antigen Processing-Deficient Vaccinia Virus-Infected Cells.

Elena Lorente, Susana Infantes, Eilon Barnea, Ilan Beer, Ruth García, Fátima Lasala,
Mercedes Jiménez, Carlos Vilches, François A. Lemonnier, Arie Admon, and Daniel
López.

J Virol. 2012 Jan;86(1):527-41.

which has been published in final form at <https://doi.org/10.1128/JVI.05737-11>

1 **MULTIPLE VIRAL LIGANDS NATURALLY PRESENTED BY DIFFERENT**
2 **CLASS I MOLECULES IN TRANSPORTER ANTIGEN PROCESSING-**
3 **DEFICIENT VACCINIA VIRUS-INFECTED CELLS**

4 Elena Lorente ¹, Susana Infantes ¹, Eilon Barnea ², Ilan Beer ³, Ruth García ¹,
5 Fátima Lasala ¹, Mercedes Jiménez ¹, Carlos Vilches ⁴, François A. Lemonnier ⁵,
6 Arie Admon ², Daniel López ^{1,*}

7
8 ¹ Centro Nacional de Microbiología, Instituto de Salud Carlos III, 28220
9 Majadahonda (Madrid), Spain. ² Department of Biology, Technion-Israel Institute
10 of Technology, Haifa 32000, Israel. ³ IBM Haifa Research Lab, Haifa, 31905,
11 Israel. ⁴ Laboratorio de Inmunogenética-HLA, Hospital Universitario Puerta de
12 Hierro, 28220 Majadahonda (Madrid), Spain. ⁵ Unité d'Immunité Cellulaire
13 Antivirale, Département d'Immunologie, Institut Pasteur, Paris Cedex 15,
14 France.

15
16 * Correspondence to: Dr. Daniel López. Unidad de Procesamiento Antigénico.
17 Centro Nacional de Microbiología. Instituto de Salud Carlos III. 28220
18 Majadahonda (Madrid), Spain. Tel: +34 91 822 37 08, FAX: +34 91 509 79 19,
19 E-mail: dlopez@isciii.es.

20 Running Title: Natural HLA ligands in TAP⁻ vaccinia-infected cells

21 Abstract word count: 202

22 Text word count: 7418

23

24 **ABSTRACT**

25 The transporter associated with antigen processing (TAP) delivers the
26 viral proteolytic products generated by the proteasome in the cytosol to the
27 endoplasmic reticulum lumen that are subsequently recognized by cytotoxic T
28 lymphocytes (CTL). However, several viral epitopes have been identified in
29 TAP-deficient models. Using mass spectrometry to analyze complex human
30 leukocyte antigen (HLA)-bound peptide pools isolated from large numbers of
31 TAP-deficient vaccinia virus-infected cells, we identified eleven ligands naturally
32 presented by four different HLA-A, -B, and -C class I molecules. Two of these
33 ligands were presented by two different HLA class I alleles, and thus, thirteen
34 different HLA/peptide complexes were formed simultaneously in the same
35 vaccinia-infected cells. In addition to the high-affinity ligands, one low-affinity
36 peptide restricted by each of the HLA-A, -B and -C class I molecules was
37 identified. Both high- and low-affinity ligands generated long-term memory CTL
38 responses against vaccinia virus in an HLA-A2 transgenic mouse model. The
39 processing and presentation of two vaccinia virus-encoded HLA-A2-restricted
40 antigens could take place via proteasomal and non-proteasomal pathways,
41 which were blocked in infected cells with chemical inhibitors specific for different
42 subsets of metalloproteinases. These data have implications for the study of the
43 effectiveness of early empirical vaccination with cowpox virus against smallpox
44 disease.

45

46 INTRODUCTION

47 The eradication of smallpox, a disease caused by variola major virus,
48 was made possible by early empirical, cross-protective vaccination with cowpox
49 virus and later through the massive worldwide production and administration of
50 vaccinia virus (VACV) (17). The *Orthopoxvirus vaccinia* is a widely used tool for
51 research and vaccine development (46), and recent concerns about
52 bioterrorism and emerging infectious diseases have elicited renewed interest in
53 VACV and other poxviruses (30). Vaccination induces a strong humoral
54 response leading to viral clearance, and the role of cellular responses in this
55 cross-protection is well documented (20)(55). In recent years, studies in both
56 vaccinated humans and human histocompatibility complex (HLA)-transgenic
57 mouse models have allowed the identification of more than 70 VACV-derived
58 epitopes restricted by various HLA molecules (reviewed in (31)(29)).

59 In cellular immunity, the recognition and killing of infected cells by CD8⁺
60 cytolytic T lymphocytes (CTLs) first requires viral proteins to be proteolytically
61 degraded (73). Antigen processing generates short peptides that are
62 translocated to the endoplasmic reticulum lumen by transporter associated with
63 antigen processing (TAP) and then assembled with newly synthesized β 2-
64 microglobulin and HLA class I heavy chain. Despite initial assumptions that the
65 multi-catalytic and ubiquitous proteasome was the only protease fully capable of
66 generating peptide ligands for presentation on HLA class I molecules, several
67 studies have demonstrated that a growing number of alternative pathways
68 contribute to endogenous antigen processing (reviewed in (12)(26)).

69 Individuals with mutations in the TAP gene that generate non-functional
70 TAP complexes have been described (reviewed in (8)). Patients with this HLA

71 class I deficiency may appear asymptomatic for long periods of their lives. TAP-
72 deficient patients do not seem particularly susceptible to viral infections or
73 neoplasms. Therefore, their immune systems must be reasonably efficient, and
74 antibodies, NK cells, CD8⁺ γδ T cells, and the reduced cytolytic CD8⁺ αβ T
75 subpopulation that is specific for TAP-independent antigens may all contribute
76 to immune defenses that protect against severe viral infections in these
77 individuals. In addition, several strains of viruses, including cowpox virus (1),
78 have found ways to obstruct TAP expression or function in order to prevent
79 CTLs from identifying infected cells (reviewed in (35)); therefore, the TAP-
80 independent pathways must be important for killing cells infected with these
81 viruses. The identification of TAP-independent epitopes conserved among
82 orthopoxviruses could also be relevant to the study of the mechanisms of early
83 empirical vaccination against smallpox disease performed with cowpox virus.

84 Although TAP-independent viral epitopes are known (reviewed in (35)),
85 there is a marked absence of methodical studies of TAP-independent
86 epitopes/ligands restricted by different HLA molecules in cells infected with a
87 single virus. Moreover, in all previous studies, very limited antigen processing
88 capacity has been reported in TAP-deficient cells. Therefore, is only one TAP-
89 independent ligand/epitope restricted by a single HLA molecule exposed on the
90 cell membrane surface, as suggested by these studies? Conversely, could a
91 TAP-deficient cell bind several viral ligands to different HLA molecules
92 simultaneously? We are interested in the identification of viral ligands presented
93 by several common HLA antigens in TAP-deficient infected cells. Using
94 immunoproteomic analysis, we compared HLA ligands isolated from large
95 numbers of healthy or VACV-infected cells. This study identified eleven TAP-

96 independent, naturally processed ligands from eight different VACV proteins in
97 infected cells that were mostly conserved among the *Orthopoxviridae* family,
98 including cowpox virus.

99

100 **MATERIALS AND METHODS**

101 *Mice*

102 H-2 class I knockout HLA-A*0201-transgenic mice (19) were bred in our
103 animal facilities in strict accordance with the recommendations in the Guide for
104 the Care and Use of Laboratory Animals of the Spanish government regulations
105 (accreditation number 28079-34A). The protocol was approved by the
106 Committee on the Ethics of Animal Experiments of the Institute of Health
107 “Carlos III” (Permit Number: PI-283). All surgery was performed under sodium
108 pentobarbital anesthesia, and all efforts were made to minimize suffering.

109 *Cell lines*

110 T2 cells, a line of TAP-deficient human cells that express HLA-A2, -B51,
111 and -Cw1 class I molecules on their surface (57), were transfected with HLA-
112 B27 (a gift from Dr. David Yu, University of California, Los Angeles, CA). The
113 mouse cell lines RMA (TAP positive) and RMA-S (TAP negative) were
114 transfected with HLA-A*0201 $\alpha 1\alpha 2$ domains, and the mouse H-2D^b $\alpha 3$
115 transmembrane and cytoplasmic domains have been previously described (51).
116 The RMA-S transfectant cells expressing HLA-B*2705 have been previously
117 described (66). All cell lines were cultured in RPMI 1640 supplemented with
118 10% fetal bovine serum and 5 μ M β -mercaptoethanol.

119 *Synthetic peptides.*

120 Peptides were synthesized in a peptide synthesizer (model 433A;
121 Applied Biosystems, Foster City, CA) and purified by reverse-phase HPLC. The

122 correct molecular mass of the peptides was established by MALDI-TOF MS,
123 and their correct composition was determined by quadrupole ion trap
124 microHPLC.

125 *Inhibitors.*

126 Brefeldin A (BFA) and all protease inhibitors were purchased from
127 Sigma-Aldrich, except for leupeptin (Amersham-UBS), pepstatin (Boehringer
128 Mannheim), Z-VAD.fmk (Enzyme System Products, CA, USA), (z-LL)₂ ketone
129 (Merck), and lactacystin (Dr. E. J. Corey, Harvard University). The specificity
130 and activity of all inhibitors used in this study were summarized in Table 1. For
131 control of activity of the protease inhibitors, RMA-HLA-A*0201 cells (1×10^8)
132 were disrupted by sonication for 15 min at 4°C, and centrifuged as previously
133 reported (39). A supernatant aliquot corresponding to 1×10^7 cells was directly
134 frozen (non-degraded control). Equivalent aliquots were incubated in the
135 presence of individual inhibitors at 200 μ M and digestion by cellular proteases
136 was allowed for 5 days at 37°C in PBS. Inhibitors were renewed daily. A sample
137 incubated without inhibitors was taken as the degraded control. After SDS-
138 PAGE separation and Coomassie Blue staining of these samples, the overall
139 protein content of each lane was quantitated by densitometry with the TINA
140 2.09e program (Isopenmeßgeräte, GmbH, Germany). % Inhibition of protein
141 degradation caused by each inhibitor was calculated as follows: $100 \times (\text{sample}$
142 $\text{with inhibitor} - \text{degraded}) / (\text{non-degraded} - \text{degraded})$.

143

144 *Infection of the T2-B27 cell line by VACV*

145 1-3 x 10⁹ T2-B27 cells were infected with VACV at a multiplicity of
146 infection of 10 plaque-forming units/cell in 10 ml, incubated for 2 h at 37°C and
147 then washed. The cells were then cultured for 24 h and stained with the
148 Omnitope antiserum-FITC that recognizes VACV purified virions. Samples were
149 analyzed by FACS. Later the cells were frozen.

150

151 *Isolation of HLA-bound peptides.*

152 HLA-bound peptides were isolated from 4 x 10¹⁰ healthy or VACV-WR-
153 infected T2-B27 transfectant cells. Cells were lysed in 1% CHAPS (Sigma), 20
154 mM Tris/HCl buffer, and 150 mM NaCl, pH 7.5, in the presence of a protease
155 inhibitor cocktail (23). HLA-peptide complexes were isolated via affinity
156 chromatography of the soluble fraction of cell extracts with the following mAbs,
157 used sequentially: PA2.1 (anti-HLA-A2) (50), ME1 (anti-HLA-B27) (13), and
158 W6/32 (specific for a monomorphic HLA class I determinant) (5) (Figure 1).
159 HLA-bound peptides were eluted at room temperature with 0.1% aqueous
160 trifluoroacetic acid (TFA), separated from the large subunits and concentrated
161 with a Centricon 3 column (Amicon, Beverly, MA) exactly as previously
162 described (23).

163 *Electrospray-ion trap mass spectrometry analysis.*

164

165 Peptide mixtures recovered after the ultra-filtration step were
166 concentrated using Micro-Tip reversed-phase columns (C₁₈, 200 µl, Harvard
167 Apparatus, Holliston, MA) (23). Each C₁₈ tip was equilibrated with 80%
168 acetonitrile in 0.1% TFA, washed with 0.1% TFA, and then loaded with the

169 peptide mixture. The tip was then washed with an additional volume of 0.1%
170 TFA, and the peptides were eluted with 80% acetonitrile in 0.1% TFA. Peptide
171 samples were then concentrated to about 18 μ l using vacuum centrifugation
172 (23).

173 HLA class I peptides immunoprecipitated with each HLA-specific mAb
174 were analyzed in three different HPLC runs by μ LC-MS/MS using an Orbitrap
175 XL mass spectrometer (Thermo Electron, San Jose, CA) fitted with a capillary
176 HPLC column (Eksigent, Dublin, CA) (23). The peptides were resolved on
177 homemade Reprosil C18 capillary columns (75 micron ID) (24) with a 7-40%
178 acetonitrile gradient for 2 h in the presence of 0.1% formic acid. The seven
179 most intense masses that exhibited single-, double-, and triple-charge states
180 were selected for fragmentation from each full mass spectrum by CID.

181

182 *Database searches.*

183

184 Sequest 3.31 (Thermo-Fisher) (14) was used for peak-list generation of
185 the μ LC-MS/MS data. The peaks were identified by using Proteome Discoverer
186 1.0 SP1 (Thermo-Fisher), combining the results of Sequest 3.31 and Bioworks
187 Browser 3.3.1 SP1 (Thermo-Fisher) (14), and using the human and virus parts
188 of the NCBI database (Jan 2009), which includes 656,486 proteins. The search
189 was not limited by enzymatic specificity, the peptide tolerance was set to 0.005
190 Da, and the fragment ion tolerance was set to 0.5 Da (23)(42). This search was
191 not limited by any methodological bias (selection of individual protein, use of
192 HLA consensus scoring algorithms, etc.). Identified peptides were selected if
193 the following criteria were met: Sequest Xcorr >1.4 for singly, >2.2 for doubly,

194 and >2.9 for triply charged peptides; P(pep) less than 1×10^{-3} ; and mass
195 accuracy of 0.005 Da (23)(42). When the MS/MS spectra fitted more than one
196 peptide, only the highest scoring peptide was analyzed. No peptides were
197 found in a search of a reversed database. The purpose of the filtering criteria
198 was to identify candidate vaccinia virus peptide MS/MS scans for further
199 manual inspection to determine whether the MS/MS fragment ion fingerprint
200 matched the identified peptide sequence. In addition, the corresponding
201 synthetic peptide was made, and its MS/MS spectrum was used to confirm the
202 assigned sequence.

203

204 *MHC/peptide stability assays.*

205

206 The following synthetic peptides were used as controls in complex
207 stability assays: KPNA2 (GLVPFLVSV, HLA-A2-restricted) (22), Flu NP
208 (SRYWAIRTR, HLA-B27-restricted) (67), HBV HBC₁₉₋₂₇ (LPSDFFPSV, HLA-
209 B51-restricted) (7), CMV pp65₇₋₁₅ (RCPEMISVL, HLA-Cw1-restricted) (32), and
210 C4CON (QYDDAVYLK, HLA-Cw4-restricted) (16). Either RMA-S transfectants
211 or T2 cells expressing low amounts of MHC class I on the cell surface were
212 incubated at 26°C for 16 h in RPMI 1640 medium supplemented with 10% heat-
213 inactivated fetal bovine serum (FBS). This allows the expression of empty MHC
214 class I molecules (without antigenic peptide) that are stable only at 26°C, but
215 not at 37°C, on the cell membrane. The cells were washed and incubated for
216 2 h at 26 °C with various concentrations of peptide in the same medium.
217 Afterward, the cells were kept at 37 °C and collected for flow cytometry after
218 4 h. This assay allows for the internalization of empty MHC class I molecules

219 and can therefore discriminate between bound and unbound peptides. HLA
220 expression levels were measured using the Abs monoclonal PA2.1 (anti-HLA-
221 A2), monoclonal ME1 (anti-HLA-B27), polyclonal H00003106-B01P (specific for
222 HLA-B class I molecules) (Abnova, Taipei, Taiwan), and polyclonal SC-19438
223 (specific for HLA-C class I molecules) (Santa Cruz Biotechnology, Santa Cruz,
224 CA) as previously described (40). Samples were acquired on a FACSCanto flow
225 cytometer (BD Biosciences, San Jose, CA, USA) and analyzed using CellQuest
226 Pro 2.0 software (BD Bioscience). Cells incubated without peptides had peak
227 fluorescence intensities close to background staining with secondary Ab alone.
228 The fluorescence index (FI) was calculated as the ratio of the mean channel
229 fluorescence of the sample to that of control cells incubated without the
230 peptides. The binding of peptides was also expressed as the EC_{50} , which is the
231 molar concentration of the peptides producing 50% of the maximum
232 fluorescence obtained at a concentration range between 0.001 and 100 μ M.

233

234 *Magnetic antigen cell separation (MACS)*

235

236 Mouse T lymphocytes were isolated by the depletion of non-T CD8⁺ cells
237 (negative selection) using the T CD8a⁺ Cell Isolation Kit (Miltenyi Biotec GmbH,
238 Gladbach, Germany) according to the manufacturer's specifications. The purity
239 of the cell preparations recovered after negative selection was verified by
240 fluorescence-activated cell sorting (FACS) and found to be higher than 95% for
241 CD8⁺ T lymphocytes (56).

242

243 *Ex vivo intracellular cytokine staining (ICS)*

244

245 Intracellular cytokine staining assays were performed as described
246 previously (58). Purified CD8⁺ T lymphocytes were obtained from HLA-A*0201
247 transgenic mice up to 30 days (memory) post i.p. infection with 1 x 10⁷ PFU
248 VACV-WR, stimulated for 2 h with either RMA or RMA-S HLA-A*0201 cells
249 infected with VACV-WR, and incubated overnight in the presence of 5 µg/ml
250 BFA. Later, cells were incubated with FITC-conjugated anti-CD8 mAb
251 (ProlImmune, Oxford, UK) for 30 min at 4°C, fixed with Intrastain kit
252 (DakoCytomation, Glostrup, Denmark) reagent A, and incubated with PE-
253 conjugated anti-IFN-γ mAb (BD PharMingen, San Diego, CA) in the presence of
254 Intrastain kit permeabilizing reagent B for 30 min at 4°C. Events were acquired
255 and analyzed as MHC/peptide stability assays.

256

257 *T cell lines, cytotoxicity assays, and ICS*

258 Polyclonal SIINFEKL or VACV peptide-monospecific CTLs were
259 generated by immunizing mice i.p. with 1 x 10⁷ PFU VACV-OVA₂₅₇₋₂₆₄ encoding
260 the miniprotein MSIINFEKL or VACV-WR as previously described (44)(39),
261 respectively. Splenocytes from immunized mice were re-stimulated *in vitro* with
262 mitomycin C-treated spleen cells pulsed with 10⁻⁶ M of the respective peptide
263 and cultured in α-MEM supplemented with 10% FBS, 1x10⁻⁷ M peptide and 1%
264 2-ME. Recombinant human interleukin-2 for the long-term propagation of
265 peptide-specific CTL lines was generously provided by Hoffmann-LaRoche. The
266 RMA-HLA-A*0201 cells were used as target cells in standard 4 h cytolytic
267 assays (39).

268 ICS assays to detect the recognition of infected cells by polyclonal CTL
269 cell lines were performed as previously described (9). CTL lines were stimulated
270 for 4 h in the presence of 5 µg/ml BFA and target cells that had been infected
271 with VACV or VACV-OVA₂₅₇₋₂₆₄ overnight. When protease inhibitors were used,
272 all drugs were added 15 min before the virus and kept at a 5-fold higher
273 concentration during the 1 hr adsorption period than throughout the infection.
274 After washing the virus inoculum, the inhibitors were kept at the concentrations
275 indicated for the individual experiments. The inhibitors were not toxic at the
276 indicated concentrations since they not affect either antigen presentation both
277 the A10L₆₈₈₋₆₉₆ and A17L₉₋₁₇ epitopes (see below) or VACV infection when the
278 Omnitope antiserum with specificity for VACV proteins from purified virions
279 (ViroStat Inc., Portland, ME) was used (Supplemental Fig. 1). The ICS with
280 polyclonal CTL was performed similarly to *ex vivo* ICS.

281

282 *In vivo cytotoxicity assay*

283 *In vivo* cytotoxicity assays were performed as published (44). Spleens
284 were obtained, erythrocytes were removed, and HLA-A*0201 splenocytes were
285 split in two populations and labeled with either a high concentration (5 µM) or a
286 low concentration (0.5 µM) of CFSE. After washing excess CFSE, CFSE^{high}
287 spleen cells were pulsed with 10⁻⁶ M VACV peptides for 30 min at 37°C. Excess
288 peptide was washed at least twice, and CFSE^{high} peptide-pulsed cells were
289 mixed with equal numbers of CFSE^{low} cells. A total of 8 × 10⁶ cells of the spleen
290 cells mixed suspension were i.p. injected into each HLA-A*0201-transgenic
291 mouse, which had been infected or not with i.p. 1 × 10⁷ PFU VACV-WR 7 days

292 earlier. Two days later, the peritoneal cavity was lavaged, and spleens were
293 extracted, and the cells were analyzed by flow cytometry to measure in vivo
294 killing, using a FACSCanto flow cytometer. Data were analyzed using CellQuest
295 Pro 2.0 software. Specific lysis was calculated as published (44) according to
296 the formula: $[1 - (\text{ratio unprimed}/\text{ratio primed}) \times 100]$, where the ratio unprimed
297 is $\%CFSE^{\text{low}}/\%CFSE^{\text{high}}$ cells remaining in control uninfected recipients, and the
298 ratio primed is $\%CFSE^{\text{low}}/\%CFSE^{\text{high}}$ cells remaining in experimental infected
299 recipients.

300

301 **RESULTS**

302

303 **VACV-specific CD8⁺ T cells recognize TAP-deficient HLA-A*0201-**
304 **transfected cells.**

305

306 As the first step in the study of TAP-independent HLA-restricted
307 responses to vaccinia virus, HLA-A*0201 transgenic mice were immunized with
308 the virus. Next, the VACV-specific CD8⁺ response was evaluated using by
309 intracellular cytokine staining (ICS) assays. A strong *ex vivo* response (50.1 ±
310 9.4% of CD8⁺ cells secreted IFN γ) specific for this virus was detected in TAP⁺
311 target cells (Fig. 2, left panel). Additionally, a small fraction of VACV-specific
312 CD8⁺ T lymphocytes recognized infected TAP-deficient cells (3.8 ± 0.8% of
313 CD8⁺ cells secreted IFN γ , Fig. 2, right panel). These data indicate the
314 existence of a TAP-independent antigen processing pathway(s) of some
315 vaccinia virus epitopes in infected cells that could be recognized by specific
316 CD8⁺ T lymphocytes.

317

318 **Physiological processing generates three different viral HLA-A2**
319 **ligands in human TAP-deficient vaccinia-infected cells.**

320

321 HLA-A2-bound peptide pools were isolated from large numbers of either
322 healthy or VACV-infected human TAP-deficient cells (110 ± 20 of MFI in VACV
323 infected cells vs 15 ± 5 in healthy cells stained with an anti-VACV antiserum).
324 These peptide mixtures were subsequently separated by reverse-phase HPLC
325 and analyzed by mass spectrometry. Using bioinformatics tools, three

326 fragmentation spectra present in the VACV-infected HLA-A2-bound peptide
327 pool, but absent from the control uninfected pool, were resolved with high
328 confidence parameters as peptides of vaccinia virus proteins. A human
329 proteome database search failed to identify any of these spectra as human
330 protein fragments, confirming the viral origin of these peptides. The first ion
331 peak, with an m/z of 926.4, was assigned to the viral amino acid sequence
332 MLDDFSAGA, spanning residues 9-17 of the A17L protein of vaccinia virus
333 (Supplemental Fig. 2, upper panel). In addition, two different ion peaks at m/z
334 974.6 and 514.8 were assigned to peptides of the same viral protein. These ion
335 peaks corresponded to SPEGEETII (Supplemental Fig. 2, medium panel) and
336 ILDRIITNA (Supplemental Fig. 2, lower panel) peptides, which span residues
337 614-623 and 688-696, respectively, of the A10L protein. Virtually all significant
338 fragments of the three MS/MS spectra were assigned as daughter ions of the
339 putative peptidic sequences (Supplemental Fig. 2). This theoretical assignment
340 was confirmed by identity with the MS/MS spectrum of the corresponding
341 synthetic peptide (Supplemental Fig. 2). Therefore, these results indicate that a
342 total of three TAP-independent HLA-A2 ligands were endogenously processed
343 and presented in the VACV-infected cells.

344

345 **Binding affinity of TAP-independent vaccinia virus ligands for the**
346 **A*0201 molecule.**

347

348 The classical anchor motifs for HLA-A*0201 binding, Leu or Met at
349 position 2 (P2) and aliphatic C-terminal residues (SYFPEITHI database:
350 <http://www.syfpeithi.de> (53)), were present in two of the three detected TAP-

351 independent viral ligands. In contrast, the ligand A10L₆₁₄₋₆₂₃ presented Pro at
352 P2, although it was co-immunoprecipitated with an HLA-A2-specific mAb and
353 thus could be an unusual HLA-A2-restricted ligand. To confirm that HLA-A*0201
354 was the MHC class I molecule that presented these ligands, MHC/peptide
355 complex stability assays were performed using TAP-deficient RMA-S cells
356 transfected with the HLA-A*0201 molecule (Fig. 3). The two viral ligands with
357 HLA-A2 anchor motifs, A10L₆₈₈₋₆₉₆ and A17L₉₋₁₇, bound to HLA-A*0201 class I
358 molecules with EC₅₀ values in the range commonly found among other natural
359 high-affinity ligands (Fig. 3B). In contrast, the HLA affinity was substantially
360 lower for the A10L₆₁₄₋₆₂₃ ligand, as the absence of HLA-A2 anchor motifs
361 suggested; therefore, this peptide must be considered a low-affinity ligand.
362 These data confirm that all ligands detected in vaccinia virus-infected cells were
363 endogenously presented in association with the A*0201 molecule.

364

365 **Three viral HLA-B*2705 ligands were endogenously processed in**
366 **human TAP-deficient vaccinia virus-infected cells.**

367

368 To date, about 60 human TAP-independent MHC class I ligands are
369 known (35)(70), and these are mostly restricted by HLA-A2 and derived from
370 the cleavage of signal sequences generated by the SPase complex. The
371 A*0201-restricted CTL epitopes of vaccinia virus that we detected in TAP-
372 deficient cells could therefore be exceptional, and TAP-independent antigen
373 processing pathways might be unable to generate vaccinia virus peptides that
374 could bind to other HLA class I molecules. HLA-B27, which was previously
375 described as an allele with high TAP dependency (2), was used to obtain

376 peptide pools from either healthy or VACV-infected TAP-deficient cells, as used
377 to identify HLA-A*0201 ligands. Again, three fragmentation spectra present in
378 the VACV-infected, HLA-B27-bound peptide pool, but absent from the control
379 uninfected pool, were also resolved as peptides of vaccinia virus proteins. The
380 human proteome database search failed to identify these spectra as human
381 protein fragments, confirming the viral origin of these HLA-B27-bound peptides.
382 The first ion peak, with an m/z of 428.8, was assigned to the viral amino acid
383 sequence SRGYFEHMKK, spanning residues 867-876 of the A10L protein of
384 vaccinia virus (Supplemental Fig. 3, upper panel), indicating that antigen
385 processing of this protein could generate several viral ligands bound to two
386 different HLA class I molecules. The second ion peak, at m/z 567.6, was
387 assigned to the peptidic sequence YRLQGFTNAGIVAYK (Supplemental Fig. 3,
388 medium panel), which spans residues 16-30 of the K2L protein. Finally, the third
389 ion peak, at m/z 471.8, corresponded to a WQTMVTN peptide (Supplemental
390 Fig. 3, lower panel), which spans residues 53-59 of the B8R protein.
391 Supplemental Fig. 3 shows that all significant fragments of these three MS/MS
392 spectra were assigned as daughter ions of the putative peptidic sequences. As
393 HLA-A2 ligands, these assignments were confirmed by identity with the MS/MS
394 spectrum of the corresponding synthetic peptide (Supplemental Fig. 3). In
395 addition, the K2L₁₆₋₃₀ ligand was also identified as a molecular ion at m/z +2
396 (Supplemental Fig. 5). Collectively, these results indicate that a similar number
397 of TAP-independent ligands were endogenously processed and presented by
398 HLA-A2 or –B27 class I molecules in the same vaccinia virus-infected cells.
399

400 **Binding affinity of TAP-independent vaccinia virus ligands for the**
401 **B*2705 molecule.**

402

403 The A10L₈₆₇₋₈₇₆ and K2L₁₆₋₃₀ (but not B8R₅₃₋₅₉) peptides have the known
404 anchor motifs for HLA-B*2705 binding Arg at P2 and basic or aliphatic C-
405 terminal residues (SYFPEITHI database (53)). As the B8R₅₃₋₅₉ peptide was also
406 co-immunoprecipitated with an HLA-B27-specific mAb, it could be an unusual
407 HLA-B27-restricted ligand. To confirm that HLA-B*2705 is the MHC class I
408 molecule that presents these ligands, MHC/peptide complex stability assays
409 were performed using TAP-deficient RMA-S cells transfected with the HLA-
410 B*2705 molecule (Figure 4). The two viral ligands with HLA-B27 anchor motifs,
411 A10L₈₆₇₋₈₇₆ and K2L₁₆₋₃₀, bound to HLA-B*2705 class I molecules with EC₅₀
412 values to similar those of other natural high-affinity ligands (Fig. 4B). In contrast,
413 the HLA affinity was substantially lower for the B8R₅₃₋₅₉ ligand, as suggested by
414 the absence of HLA-B27 anchor motifs, and this peptide could be considered a
415 low-affinity ligand. These data confirm that the ligands detected in vaccinia
416 virus-infected cells were endogenously presented in association with the
417 B*2705 molecule. In summary, either HLA-A*0201 or B*2705 class I molecules
418 can bind both high- and low-affinity ligands derived from different vaccinia virus
419 proteins.

420

421 **Six vaccinia virus ligands were endogenously presented by HLA-**
422 **B51 and/or –Cw1 class I molecules in human TAP-deficient cells.**

423

424 Given that several TAP-independent viral ligands were identified in
425 association with either HLA-A*0201 or B*2705 class I molecules (see above),
426 we investigated the possibility of new vaccinia virus ligands being presented by
427 other HLA class I molecules expressed in the same T2 cells. As in the previous
428 two analyses, six fragmentation spectra were found in the VACV-infected
429 peptide pool that were absent from the uninfected control pool, and these
430 spectra were also resolved as peptides of vaccinia virus proteins. Furthermore,
431 the human proteome database search also failed to identify these spectra as
432 human protein fragments, confirming the viral origin of these HLA-bound
433 peptides. Supplemental Figures 4 and 5 show the experimentally obtained
434 MS/MS spectra and their respective assignments. Each putative peptidic
435 sequence was confirmed by identity with the MS/MS spectrum of the
436 corresponding synthetic peptide (Supplemental Fig. 4 and 5). Five of these
437 peptides were new viral sequences: IAMKRTLLEL (D5R₁₄₈₋₁₅₇), LPFGSLGI
438 (A50R₂₉₄₋₃₀₁), IPSPGIMLV (C11R₁₀₁₋₁₁₀), MLDDFSAGAGVLDKDL (A17L₉₋₂₅),
439 and DGLIISI (D8L₁₁₂₋₁₁₉). Surprisingly, the K2L₁₆₋₃₀ ligand previously detected
440 in association with HLA-B*2705 (Supplemental Figure 3) was also
441 immunoprecipitated in the third round with the W6/32 Ab. As HLA-A2, - B51,
442 and -Cw1 present peptides with similar anchor motifs (SYFPEITHI database,
443 (53)), HLA/peptide complex stability assays were performed to confirm that the
444 sequential immunoprecipitation was performed correctly and to exclude the
445 possibility that residual HLA-A2-bound ligands that were not fully
446 immunoprecipitated with the PA2.1 (anti-HLA-A2) Ab in the first round would be
447 immunoprecipitated in the third round with the W6/32 Ab (specific for a
448 monomorphic HLA class I determinant). Figure 5A shows that, in contrast to the

449 positive control KPNA2 peptide, binding of HLA-A2 complexes to these six
450 ligands was not detected. Therefore, these viral ligands do not bind to HLA-A2,
451 which validates the experimental strategy used. In addition, to identify the HLA
452 restriction of these ligands, new HLA/peptide complex stability assays using
453 TAP-deficient T2 cells with specific anti-HLA-B or -C Abs were performed. The
454 numbers of HLA-peptide surface complexes induced by the IAMKRTLLEL
455 (D5R₁₄₈₋₁₅₇), LPFGSLGI (A50R₂₉₄₋₃₀₁), and IPSPGIMLV (C11R₁₀₁₋₁₁₀) synthetic
456 peptides were similar to those induced by a well-known HLA-B51 ligand, HBV
457 HBC₁₉₋₂₇ (Fig. 5B), using the anti-HLA-B Ab, indicating that these peptides were
458 restricted by the HLA-B51 class I molecule. HLA stabilization was detected
459 using anti-HLA-C (Fig. 5C) Ab with IPSPGIMLV (C11R₁₀₁₋₁₁₀),
460 MLDDFSAGAGVLDKDL (A17L₉₋₂₅), and DGLIISI (D8L₁₁₂₋₁₁₉), indicating that
461 these peptides are restricted by the HLA-Cw1 allele. In addition, the K2L₁₆₋₃₀
462 ligand also bound to HLA-B*2705 (Supplemental Fig. 3 and Figure 4) was
463 positive in their binding to HLA-Cw1 class I molecule justifying their dual
464 immunoprecipitation (Figure 5). Five of these six viral ligands bound to HLA-B51
465 (Fig. 5D) or –Cw1 (Fig. 5E) class I molecules with EC₅₀ values similar to those
466 of other natural high-affinity ligands. The only exception was the K2L₁₆₋₃₀
467 peptide, which showed a substantially lower affinity for HLA-Cw1, indicating that
468 this peptide could be considered a low-affinity ligand (Fig. 5E).

469

470 **Thirteen natural peptide-HLA class I complexes were formed**
471 **simultaneously in the same infected TAP-deficient cells.**

472

473 A total of eleven viral ligands were identified bound to the four HLA class
474 I molecules expressed in the T2 cells (summarized in Table 2). Similar numbers
475 of ligands (3 or 4) were identified in association with HLA class I molecules
476 previously described as having low (HLA-A2), high (HLA-B27) or unknown
477 (HLA-B51 and –Cw1) TAP dependency. The same N-terminal core peptide,
478 MLDDFSAGA, was found in two different ligands, A17L₉₋₁₇ and A17L₉₋₂₅, bound
479 to HLA-A2 and –Cw1, respectively. Ten sequences were new vaccinia HLA
480 ligands. Most were restricted by a single HLA allele, but two ligands, K2L₁₆₋₃₀
481 and C11R₁₀₁₋₁₁₀, were found to be associated with two different alleles, HLA-
482 B27 and –Cw1 or HLA-B51 and –Cw1, respectively. This implies that thirteen
483 different natural peptide-HLA class I complexes were formed simultaneously in
484 the same infected TAP-deficient cells.

485 **Conservation of ligands among the *Orthopoxvirus* family.**

486 The sequences of eleven vaccinia virus ligands identified in the WR
487 strain were compared with homologs derived from various poxviruses. This
488 comparison included the Copenhagen and MVA strains of VACV, two strains of
489 human poxvirus (variola major and variola minor), and other mammalian
490 poxviruses, such as camelpox, cowpox, ectromelia virus, horsepox,
491 monkeypox, rabbitpox, and taterapox. This study revealed the high degree of
492 conservation of the ligands among orthopoxviruses (Table 3). Ten of these
493 eleven ligands are almost fully conserved in the variola major and minor
494 viruses, with a minor substitution in the P7 position of the C11R₁₀₁₋₁₁₀ sequence.
495 Only 60% of the previously described TAP⁺ vaccinia virus epitopes are
496 conserved in the variola proteome (49)(52)(45) , indicating that TAP-

497 independent vaccinia ligands are more highly conserved than TAP-dependent
498 epitopes between immunogenic and pathologic poxviruses.

499 **Low hydrophobicity in TAP-independent vaccinia virus ligands.**

500 Eight TAP-independent epitopes, restricted by four different HLA class I
501 molecules, were previously characterized in the Epstein-Barr virus (EBV) CTL
502 response (reviewed in (37)). For this virus, only peptides from the BRLF1 and
503 LMP2 proteins with high hydrophobicity are TAP independent (36)(37).
504 Therefore, we tested this correlation in our vaccinia virus system. The
505 hydrophobicity of all TAP-independent EBV epitopes was up to 2.1 on the grand
506 average of hydropathicity (GRAVY) scale, with the maximum value found for the
507 EBV LMP2 LLWTLVVLL peptide (Table 4). All three HLA-B*2705 ligands and
508 the A10L₆₁₄₋₆₂₃ HLA-A*0201-restricted ligand identified in our study were
509 hydrophilic, with negative GRAVY values (Table 4). Only the vaccinia virus
510 HLA-Cw1-restricted epitope D8L₁₁₂₋₁₁₉, with a GRAVY value of 2.1, was
511 hydrophobic. The other six ligands showed low positive GRAVY values,
512 indicating low hydrophobicity (Table 4). The GRAVY mean of these eleven
513 vaccinia ligands was only 0.3, which was very different from the EBV epitopes
514 and more similar to the TAP-dependent vaccinia epitopes (Table 4). These
515 results show that hydrophobicity is not a necessary condition for the TAP-
516 independent presentation of ligands/epitopes from other viruses such as
517 vaccinia.

518

519 **Recognition of HLA-A*0201 ligands by specific CD8⁺ T cells in HLA**
520 **transgenic mice immunized with vaccinia virus.**

521

522 To study the immunogenicity of the identified HLA-A*0201 viral ligands,
523 transgenic HLA-A*0201-positive mice were immunized with VACV. Later,
524 physiological measure of the functional in vivo activity of CD8⁺ T lymphocytes
525 against HLA-A2 viral ligand identified by mass spectrometry was carried out.
526 HLA-A*0201-transgenic mice eliminated VACV peptide-pulsed CFSE^{high} cells
527 when they had been previously immunized but not with uninfected control
528 VACV (Fig. 6). In addition, up to 30 days post-immunization, polyclonal CTL
529 lines were generated that were monospecific for each HLA-A2 viral ligand
530 identified by mass spectrometry. These CTL lines specifically recognized
531 peptide-pulsed cells (Fig. 7), indicating that the HLA ligands were all A*0201-
532 restricted CTL epitopes and that they were simultaneously recognized as part of
533 the long-term memory response to vaccinia virus. Also, these CD8⁺ effector
534 lines also specifically recognized VACV-infected cells (Figure 7D).

535 Several attempts to induce CTL responses in HLA-B*2705 transgenic
536 mice against the viral B*2705-restricted ligands identified were unsuccessful.
537 This was also the case for the influenza NP epitope previously described in flu-
538 infected B27⁺ humans (67) that we used as a CTL-positive control. The mouse
539 model used carried HLA-B27 and endogenous murine H2 class I molecules
540 (27), in contrast to the HLA-A2 transgenic mouse knockout used previously for
541 these mouse molecules (51). This may reduce the efficiency of HLA-restricted
542 Ag-specific responses to undetectable levels (10) although the T cell repertoire
543 as limiting factor could not be discarded. Unfortunately, HLA-B27 transgenic
544 mice deficient for H2 class I expression (10) were not available. Therefore, the

545 study of HLA-B*2705-restricted CTL responses against vaccinia virus ligands
546 was not feasible.

547

548 **Three different antigen processing pathways were involved in**
549 **the presentation of A10L₆₈₈₋₆₉₆ and A17L₉₋₁₇ epitopes in infected TAP-**
550 **sufficient cells.**

551

552 To study the antigen processing pathways involved in the endogenous
553 generation of the A10L₆₈₈₋₆₉₆ and A17L₉₋₁₇ viral epitopes, we investigated the
554 presentation of these epitopes to specific CTL in the presence of diverse
555 protease inhibitors in VACV-infected TAP-sufficient cells.

556 First, to demonstrate that these HLA-A2-restricted epitopes require
557 endogenous processing, their presentation was analyzed in the presence of
558 BFA. This drug blocks class I export beyond the cis-Golgi compartment (38),
559 thus preventing the surface expression of newly assembled HLA class I-peptide
560 complexes from endogenous origin (Table 1 summarizes the specificity of all
561 inhibitors used). The complete inhibition of specific lysis in both specific CTL
562 lines caused by the addition of BFA during vaccinia infection (Fig. 8A),
563 demonstrated that the two relevant epitopes were indeed generated from
564 proteins endogenously processed in infected cells.

565 Lactacystin (LC), a *Streptomyces* metabolite (18)(48) was used to study
566 the involvement of the proteasome in the presentation of these epitopes. This
567 drug had no effect on the specific recognition of target cells infected with VACV
568 by A10L₆₈₈₋₆₉₆- or A17L₉₋₁₇-specific CTLs (Fig. 8A). Although the proteasome

569 may be involved in the antigen processing of these epitopes, these data
570 suggest that the LC-inhibitable proteasome activity is not absolutely required.

571 Because several endogenous TAP-independent HLA-2 class I ligands
572 are derived by cleavage of the signal sequences generated by the signal
573 peptidase (SPase) complex (35)(70) and because no specific inhibitor of this
574 enzymatic activity was available, the involvement of SPase complex in A17L₉₋₁₇
575 ligand production could not be studied directly. SPase-processed peptides need
576 further cleavage by signal peptide peptidase (SPPase) (69)(68)(41). Therefore,
577 the involvement of SPPase in antigen presentation was tested by treating target
578 cells with the SPPase-specific inhibitor (z-LL)₂ ketone (69)(68){. Similarly to LC,
579 the inhibition of specific presentation was not detected with this drug (Fig. 8A).

580 To identify proteases distinct from the proteasomes that could contribute
581 to antigen processing of both HLA-A2 epitopes, experiments with several
582 specific protease inhibitors were performed. Leupeptin (LEU) {Umezawa, 1976
583 19523 /id}, pepstatin (PEPST) (33)(65) and 1,10-phenanthroline (PHE)
584 (33)(64) were initially tested because they specifically inhibit different protease
585 families (Table 1), thereby covering a wide range of proteases. Figure 8A shows
586 that these three inhibitors had no effect on the specific recognition of target cells
587 infected with VACV. In addition, because the activity of ERAAP, an enzyme
588 involved in antigen processing (59)(72), is not fully blocked by PHE at the
589 concentration used in this study, leucinethiol (LeuSH) (Table 1) (61) was also
590 included. Like the other protease inhibitors, LeuSH did not inhibit the recognition
591 of infected cells (Fig. 8A), indicating that ERAAP cannot be involved in the
592 generation of these TAP-independent epitopes.

593 In summary, the inhibitors used did not block the presentation of the two
594 viral epitopes tested. The two most likely explanations for these results are as
595 follows. First, these epitopes could be processed by protease(s) that not were
596 blocked by the collection of inhibitors used in Figure 8A. This explanation is not
597 likely because the inhibitors were chosen to cover a wide range of protease
598 classes. Alternatively, these epitopes could be processed in parallel by different
599 proteases independently, meaning that the different antigen processing
600 pathways would need to be inhibited at the same time to see an effect. To test
601 this hypothesis, the effects of combinations of several inhibitors on antigen
602 presentation in vaccinia infected cells were tested.

603 Because most class I epitopes are generated by proteasome activity, the
604 presentation of these epitopes was analyzed in the presence of LC, together
605 with each other inhibitor in turn. Figure 8B shows that the combination of LC
606 with (z-LL)₂ ketone, LEU, or PEPST did not block presentation in infected cells.
607 In contrast, a partial block of presentation was observed in target cells treated
608 with LC and PHE (Fig. 8B). These results demonstrate that the A10L₆₈₈₋₆₉₆ and
609 A17L₉₋₁₇ peptides were processed by both metalloproteases and proteasomes
610 in vivo. Additionally, the antigen presentation of both epitopes was partially
611 inhibited by the combination of LC and LeuSH, indicating that ERAAP or other
612 metallo-aminopeptidases were involved in the generation of these viral
613 epitopes. Metallopeptidases can be divided into aminopeptidases,
614 endopeptidases, carboxypeptidases, and carboxy-dipeptidases, among others,
615 based on their cleavage mechanism (reviewed in (54)). Some of these groups
616 can be distinguished by the use of different specific inhibitors (summarized in
617 Table 1). To more precisely identify the metallopeptidase group involved in both

618 A10L₆₈₈₋₆₉₆ and A17L₉₋₁₇ antigen processing, target cells were infected with
619 VACV and treated with a mixture of LC and different specific inhibitors (Table
620 1). The caspase-1-specific inhibitor z-VAD.fmk was also included in view of the
621 sensitivity of this cysteine protease to PHE. Remarkably, none of the different
622 combinations of inhibitors tested prevented antigen presentation to specific
623 CTLs (Fig. 8B). Because phosphoramidon is able to inhibit bacterial
624 endopeptidases but does not block all metallo-endopeptidases of mammalian
625 origin, the most likely explanation for our results is that mammalian metallo-
626 endopeptidases that are not blocked by phosphoramidon are involved in the
627 antigen processing of these viral epitopes. Over 100 different well-characterized
628 higher vertebrate metallo-endoproteases are resistant to this drug (6); therefore,
629 positive identification of the peptidase involved the processing of TAP-
630 independent vaccinia epitopes awaits further characterization.

631 To demonstrate that two different metalloproteases, amino and endopeptidases,
632 were independently involved in the generation of the A10L₆₈₈₋₆₉₆ and A17L₉₋₁₇
633 epitopes, their presentation was analyzed in the presence of a mixture of PHE
634 and LeuSH. The incomplete block detected in presentation indicates that
635 aminometalloproteases and metallo-endopeptidases are independently needed
636 to process both the A10L₆₈₈₋₆₉₆ and A17L₉₋₁₇ epitopes (Fig. 8B). Lastly, the
637 recognition of infected cells by specific CTL was abrogated in the presence of
638 three inhibitors: LC, PHE and LeuSH (Fig. 8B). To exclude that the inhibitory
639 effects of LC, PHE or LeuSH were due to toxic effects on target cells or on rVV
640 replication, rather than to a specific block of the respective proteases, similar
641 experiments in the same target cells to those shown in Fig. 8B were performed
642 in parallel using the VACV-OVA₂₅₇₋₂₆₄ which codes for the miniprotein

643 MSIIINFEKL. Specific recognition by SIINFEKL-specific CTL of target cells
644 infected with the VACV-OVA₂₅₇₋₂₆₄ virus (64 ± 11 % of CD8⁺ cells secreted
645 IFN γ) was detected. In contrast, VACV-OVA₂₅₇₋₂₆₄-infected target cells
646 incubated with all combinations of these three inhibitors were efficiently
647 recognized by SIINFEKL-specific CTL and no inhibition was detected (hatched
648 bars in Fig. 8B). These data indicate that inhibition of the A10L₆₈₈₋₆₉₆ and A17L₉₋
649 ₁₇ epitopes by addition of LC, PHE and LeuSH drugs is formally due to specific
650 blockage of the respective proteases and not to a block in rVV replication or
651 other toxic effects.

652 In summary, the proteasome, aminometalloproteases, and metallo-
653 endopeptidases are all independently involved in the antigen processing of both
654 A10L₆₈₈₋₆₉₆ and A17L₉₋₁₇ epitopes. The existence of identical neighboring
655 residues around both the A10L₆₈₈₋₆₉₆ and A17L₉₋₁₇ sequences (Fig. 8C) could
656 explain the similarity of the antigen processing pathways identified in these two
657 different HLA-restricted epitopes.

658

659

DISCUSSION

660 The results reported here show an exceptional diversity of TAP-
661 independent ligands, with eleven ligands processed and presented as part of
662 thirteen different HLA/peptide complexes simultaneously in VACV-infected cells.
663 All three of the identified HLA-A2 ligands generated long-term CTL memory
664 responses against vaccinia virus in a transgenic mouse model. Proteasomal
665 and non-proteasomal pathways were involved in the processing and
666 presentation of two vaccinia virus-encoded HLA-A2-restricted antigens.

667 Identification of viral HLA ligands by mass spectrometry analysis
668 contributes to a better understanding of the cellular antiviral immune response.
669 However, the mass spectrometry strategies to identify such ligands have not
670 become routine because of the difficulty in selecting and identifying the very
671 limited number of viral sequences among the large number of self-peptides
672 bound to HLA class I molecules. Therefore, the number of studies on viral HLA
673 ligands is still limited. To date, only two studies have identified vaccinia virus
674 ligands by mass spectrometry (45)(25). Currently, we identified three to four
675 TAP-independent ligands that were processed and presented by each of the
676 four class I molecules expressed in infected cells. Neither HLA-specific elution
677 nor CTL responses have previously been reported in TAP⁺ cells for ten of the
678 ligands identified in our study. However, as all three TAP-independent HLA-
679 A*0201 ligands also generated responses in TAP⁺ HLA-A*0201-transgenic
680 mice, these epitopes must also be generated in wild-type cells.

681 We detected HLA ligands from viral gene products expressed in the three
682 gene expression temporality clusters of the viral life cycle (Supplemental Table
683 1), early (A50R, B8R, C11R, and D5R), early/late (K2L), and late (A10L, A17L,
684 and D8L), in agreement with a previous study investigating the CTL response in
685 the same virus strain (52). Similar to the TAP⁺ response, the TAP-independent
686 response also sampled proteins from the entire viral life cycle of the VACV WR
687 strain. Other authors reported the absence of presentation of peptides derived
688 from late viral Ags to specific T cells by infected mouse target cells (28)(45), but
689 a different VACV strain was used in their studies. The sequences we identified
690 were derived from eight different vaccinia virus proteins (Supplemental Table 1).
691 Five of these proteins present signal sequence or transmembrane domains in
692 their respective amino acid sequences and are therefore accessible to HLA-
693 containing compartments where they could be processed by resident proteases.
694 In contrast, for three vaccinia proteins, A10L, A50R, and D5R, no obvious TAP-
695 independent antigen presentation could be predicted. However vaccinia DNA
696 replication is associated with the cytoplasmic side of the rough ER, and when
697 the replication proceeds, ER membranes are recruited (reviewed in (60)). Late
698 in infection, the ER envelope is disassembled, and these membranes are
699 recycled to the ER (reviewed in (60)). During this complex process that includes
700 deep membrane reorganization, some molecules of A10L, A50R, and D5R
701 proteins could gain access to a TAP-independent antigen processing pathway.

702 In most cases, the identified natural MHC class I ligands had the
703 canonical anchor motifs, and their respective antigenicity and MHC class I
704 binding affinity were correlated. This suggests that only high-affinity peptides
705 are recognized by CTLs and that epitopes of low affinity may be

706 immunologically irrelevant. We have demonstrated that cytotoxic responses are
707 targeted against both high- and low-affinity HLA-A*0201 ligands of VACV;
708 therefore, the TCRs of individual CTLs specific for low-affinity epitopes must
709 display a compensatory high affinity. In addition, it has been reported that low-
710 affinity self-peptides in autoimmunity (reviewed in (15)) or tumor peptides (3)
711 generate specific responses. These findings suggest that the range of peptides
712 that can generate CTLs is broader than formerly considered and that the role of
713 low-affinity epitopes in antiviral responses must be evaluated in future studies.

714 Different MHC class I alleles have different TAP dependencies. The
715 widespread HLA-A2 allele is considered to be the least TAP dependent (63).
716 Alleles such as HLA-B7 and –B8 can also bind ligands that are dependent on
717 mechanisms other than TAP transport, while other MHC class I molecules,
718 including HLA-A3, -A24, and –B27, have been described as mainly TAP
719 dependent (2). In the present report, several TAP-independent ligands were
720 identified for alleles with different TAP requirements. Thus, the overall
721 expression of MHC class I molecules with endogenous bound peptides is not
722 indicative of specific TAP-independent cellular responses, which must be
723 studied individually in each specific virus.

724 Although TAP-independent viral epitopes are known (reviewed in
725 (12):(26):(35)), only one epitope has been identified as the target of a specific
726 antiviral CTL response in most of the cases studied. No systematic studies of
727 TAP-independent pathways with a single virus and different HLA molecules
728 have been reported. The exception is EBV, for which CTLs from different
729 donors recognize several viral epitopes from two different viral proteins
730 restricted by several HLA class I molecules in TAP-negative cell backgrounds

731 (reviewed in (37)). Here, we report a second case with eleven ligands from eight
732 different viral proteins presented by four different HLA class I molecules in the
733 same TAP-deficient vaccinia-infected cells. The simultaneous presentation of
734 this broad complexity of viral peptide/MHC complexes can help to explain why
735 TAP-deficient patients do not seem particularly susceptible to viral infections
736 and may appear asymptomatic for long periods of their lives. In addition, the
737 existence of multiple TAP-independent ligands in two very different viruses, a
738 gamma-herpes virus and an orthopoxvirus, suggests that these pathways could
739 be an extended, but perhaps secondary, mechanism that forms part of the
740 multiple layers of defense against viral infection and that the significance of
741 these alternative processing pathways *in vivo* needs to be further studied.

742 The involvement of the following proteases in the processing of
743 endogenously synthesized antigens, independently of the classical proteasome
744 pathway, has been reported previously (reviewed in (11)). In the present report,
745 two HLA-A2-restricted epitopes could be processed in parallel by amino
746 metallo-peptidases as well as metallo-endoproteases and a classic proteasomal
747 pathway.

748 In addition to the A17L₉₋₁₇ epitope previously described in TAP-sufficient
749 cells (4), two distinct peptide epitopes recognized by human HLA-A2-restricted
750 CD8⁺ T cells and eight HLA-B27, -B51, and/or -Cw1 ligands were newly
751 detected in this study. Nine of the viral ligands identified are conserved in all
752 three vaccinia virus strains, seven orthopoxviruses (including cowpox virus) and
753 two variola strains. In contrast, only 60% of the previously described vaccinia
754 virus epitopes are identical in the variola proteome (49)(52)(45). Therefore,
755 TAP-independent vaccinia ligands are more highly conserved than TAP-

756 dependent epitopes between immunogenic and pathologic poxviruses and
757 could be more specific targets for immunization. Cowpox virus, the first
758 component of early vaccines, specifically inhibits TAP-dependent peptide
759 translocation(1); therefore, TAP-independent epitopes conserved between
760 variola and this virus are probably responsible for the initial cross-protection.
761 Additionally, truncated gene fragments similar to TAP-blocking CPXV12 protein
762 are widely found in poxviral genomes (Poxvirus Bioinformatics Resources
763 Center, <http://www.poxvirus.org>) and frequently represent loss-of-function
764 phenotypes, but this “genetic debris” might acquire entirely new, unanticipated
765 functions. Therefore, the conservation of epitopes between different vaccine
766 strains and pathogens is relevant for vaccine design and suggests that ligands
767 from TAP-independent pathways could be interesting candidates to be included
768 in immunization protocols. This is also important with respect to bioterrorism
769 because some countries did not participate in the WHO smallpox eradication
770 program, and at the present time, no information about the elimination of their
771 samples of the pandemic virus has been reported.

772 Computational methods for predicting MHC-peptide binding are
773 increasingly being used to identify epitopes for vaccine design and to monitor T
774 cell responses (reviewed in (34)(43)). The prediction of MHC-peptide binding is
775 far from perfect, as our results indicate. The prediction by bioinformatics tools of
776 HLA class I molecules presenting the nine vaccinia viral ligands identified in
777 current study showed several different mistakes, including incomplete HLA
778 identification (K2L₁₆₋₃₀ and C11R₁₀₁₋₁₁₀ ligands), ambiguous HLA restriction
779 (D5R₁₄₈₋₁₅₇ and A17L₉₋₂₅ ligands) or the wrong assignation (A10L₆₁₄₋₆₂₃ and
780 D8L₁₁₂₋₁₁₉ ligands) (Table 5). In summary, more than half of these ligands

781 showed inconsistencies between the computational predictions and
782 experimentally detected HLA restriction. These results reveal the limitations of
783 predictive methods for identifying natural MHC class I ligands and T cell
784 epitopes. The current analytical algorithms may not be sufficiently accurate and
785 should be used with caution.

786 Collectively, the results in the current report highlight the importance of
787 analyzing natural peptides that result from the endogenous processing of viral
788 proteins and demonstrate the complexity and plasticity of MHC-peptide
789 interactions. This analysis is of fundamental importance for gaining a detailed
790 understanding of MHC class I-restricted immunity and future vaccine design.

791

792

793 ACKNOWLEDGEMENTS

794 We thank Dr. J. A. López de Castro (Centro de Biología Molecular
795 Severo Ochoa, Madrid, Spain) for the cell lines. Recombinant human
796 interleukin-2 was generously provided by Hoffmann-LaRoche.

797 This work was supported by grants to D. L. from the Programa Ramón y
798 Cajal, and the FIPSE Foundation and to A. A. from the ISF 916/05. The funders
799 had no role in study design, data collection and analysis, decision to publish, or
800 preparation of the manuscript. The authors have no conflicting financial
801 interests.

802

803 **REFERENCES**

- 804 1. **Alzhanova, D., D. M. Edwards, E. Hammarlund, I. G. Scholz, D.**
805 **Horst, M. J. Wagner, C. Upton, E. J. Wiertz, M. K. Slifka, and K. Fruh.**
806 2009. Cowpox virus inhibits the transporter associated with antigen
807 processing to evade T cell recognition. *Cell Host. Microbe* **6**:433-445.
- 808 2. **Anderson, K. S., J. Alexander, M. Wei, and P. Cresswell.** 1993.
809 Intracellular transport of class I MHC molecules in antigen processing
810 mutant cell lines. *J Immunol.* **151**:3407-3419.
- 811 3. **Apostolopoulos, V., V. Karanikas, J. S. Haurum, and I. F. McKenzie.**
812 1997. Induction of HLA-A2-restricted CTLs to the mucin 1 human breast
813 cancer antigen. *J Immunol.* **159**:5211-5218.
- 814 4. **Assarsson, E., J. Sidney, C. Oseroff, V. Paschetto, H. H. Bui, N.**
815 **Frahm, C. Brander, B. Peters, H. Grey, and A. Sette.** 2007. A
816 quantitative analysis of the variables affecting the repertoire of T cell
817 specificities recognized after vaccinia virus infection. *J Immunol.*
818 **178**:7890-7901.
- 819 5. **Barnstable, C. J., W. F. Bodmer, G. Brown, G. Galfre, C. Milstein, A.**
820 **F. Williams, and A. Ziegler.** 1978. Production of monoclonal antibodies
821 to group A erythrocytes, HLA and other human cell surface antigens-new
822 tools for genetic analysis. *Cell* **14**:9-20.
- 823 6. **Barrett, A. J.** 2004. Metallopeptidases, p. 231-1047. *In* A. J. Barrett, N.
824 D. Rawlings, and J. F. Woessner (eds.), *Handbook of Proteolytic*
825 *Enzymes.* Academic Press, London.
- 826 7. **Bertoni, R., J. Sidney, P. Fowler, R. W. Chesnut, F. V. Chisari, and A.**
827 **Sette.** 1997. Human histocompatibility leukocyte antigen-binding
828 supermotifs predict broadly cross-reactive cytotoxic T lymphocyte
829 responses in patients with acute hepatitis. *J Clin Invest* **100**:503-513.
- 830 8. **Cerundolo, V. and H. de la Salle.** 2006. Description of HLA class I- and
831 CD8-deficient patients: Insights into the function of cytotoxic T
832 lymphocytes and NK cells in host defense. *Semin. Immunol.* **18**:330-336.
- 833 9. **Chen, W., L. C. Anton, J. R. Bennink, and J. W. Yewdell.** 2000.
834 Dissecting the multifactorial causes of immunodominance in class I-
835 restricted T cell responses to viruses. *Immunity.* **12**:83-93.
- 836 10. **Cheuk, E., C. D'Souza, N. Hu, Y. Liu, H. Lang, and J. W.**
837 **Chamberlain.** 2002. Human MHC class I transgenic mice deficient for
838 H2 class I expression facilitate identification and characterization of new
839 HLA class I-restricted viral T cell epitopes. *J Immunol.* **169**:5571-5580.
- 840 11. **Del Val, M., S. Iborra, M. Ramos, and S. Lázaro.** 2011. Generation of
841 MHC class I ligands in the secretory and vesicular pathways. *Cell. Mol.*
842 *Life Sci.* **in press.**

- 843 12. **Del Val, M. and D. López.** 2002. Multiple proteases process viral
844 antigens for presentation by MHC class I molecules to CD8⁺ T
845 lymphocytes. *Mol. Immunol.* **39**:235-247.
- 846 13. **Ellis, S. A., C. Taylor, and A. McMichael.** 1982. Recognition of HLA-
847 B27 and related antigen by a monoclonal antibody. *Hum. Immunol.* **5**:49-
848 59.
- 849 14. **Eng, J., A. McCormack, and J. Yates.** 2009. An approach to correlate
850 tandem mass spectral data of peptides with amino acid sequences in a
851 protein database. *J. Amer. Soc. Mass. Spect.* **5**:976-989.
- 852 15. **Fairchild, P. J. and D. C. Wraith.** 1996. Lowering the tone: mechanisms
853 of immunodominance among epitopes with low affinity for MHC.
854 *Immunol. Today* **17**:80-85.
- 855 16. **Fan, Q. R., D. N. Garboczi, C. C. Winter, N. Wagtmann, E. O. Long,**
856 **and D. C. Wiley.** 1996. Direct binding of a soluble natural killer cell
857 inhibitory receptor to a soluble human leukocyte antigen-CW4 class I
858 Major Histocompatibility Complex molecule. *Proc. Natl. Acad. Sci. U. S.*
859 *A.* **93**:7178-7183.
- 860 17. **Fenner, F., D. A. Henderson, I. Arita, Z. Jezek, and I. Ladnyi.** 2004.
861 *Smallpox and Its Eradication.* (W. H. O. , Geneva).
- 862 18. **Fenteany, G., R. F. Standaert, W. S. Lane, S. Choi, E. J. Corey, and**
863 **S. L. Schreiber.** 1995. Inhibition of proteasome activities and subunit-
864 specific amino-terminal threonine modification by lactacystin. *Science*
865 **268**:726-731.
- 866 19. **Firat, H., F. Garcia-Pons, S. Tourdot, S. Pascolo, A. Scardino, Z.**
867 **Garcia, M. L. Michel, R. W. Jack, G. Jung, K. Kosmatopoulos, L.**
868 **Mateo, A. Suhrbier, F. A. Lemonnier, and P. Langlade-Demoyen.**
869 1999. H-2 class I knockout, HLA-A2.1-transgenic mice: a versatile animal
870 model for preclinical evaluation of antitumor immunotherapeutic
871 strategies. *Eur. J Immunol* **29**:3112-3121.
- 872 20. **Freed, E. R., R. J. Duma, and M. R. Escobar.** 1972. *Vaccinia necrosum*
873 and its relationship to impaired immunologic responsiveness. *Am. J.*
874 *Med.* **52**:411-420.
- 875 21. **Howell, S., A. M. Caswell, A. J. Kenny, and A. J. Turner.** 1993.
876 Membrane peptidases on human osteoblast-like cells in culture:
877 hydrolysis of calcitonin and hormonal regulation of endopeptidase- 24.11.
878 *Biochem. J.* **290**:159-164.
- 879 22. **Hunt, D. F., R. A. Henderson, J. Shabanowitz, K. Sakaguchi, H.**
880 **Michel, N. Sevilir, A. L. Cox, E. Appella, and V. H. Engelhard.** 1992.
881 Characterization of peptides bound to the class I MHC molecule HLA-
882 A2.1 by mass spectrometry. *Science* **255**:1261-1263.

- 883 23. **Infantes, S., E. Lorente, E. Barnea, I. Beer, J. J. Cragnolini, R.**
884 **García, F. Lasala, M. Jiménez, A. Admon, and D. López.** 2010.
885 Multiple, non-conserved, internal viral ligands naturally presented by
886 HLA-B27 in human respiratory syncytial virus-infected cells. *Mol. Cell.*
887 *Proteomics* **9**:1533-1539.
- 888 24. **Ishihama, Y., J. Rappsilber, J. S. Andersen, and M. Mann.** 2002.
889 Microcolumns with self-assembled particle frits for proteomics. *J*
890 *Chromatogr. A* **979**:233-239.
- 891 25. **Johnson, K. L., I. G. Ovsyannikova, C. J. Mason, H. R. Bergen, III,**
892 **and G. A. Poland.** 2009. Discovery of naturally processed and HLA-
893 presented class I peptides from vaccinia virus infection using mass
894 spectrometry for vaccine development. *Vaccine* **28**:38-47.
- 895 26. **Johnstone, C. and M. Del Val.** 2007. Traffic of proteins and peptides
896 across membranes for immunosurveillance by CD8⁺ T Lymphocytes: A
897 topological challenge. *Traffic* **8**:1486-1494.
- 898 27. **Kalinke, U., B. Arnold, and G. J. Hammerling.** 1990. Strong
899 xenogeneic HLA response in transgenic mice after introducing an alpha
900 3 domain into HLA B27. *Nature* **348**:642-644.
- 901 28. **Kastenmuller, W., G. Gasteiger, J. H. Gronau, R. Baier, R. Ljapoci, D.**
902 **H. Busch, and I. Drexler.** 2007. Cross-competition of CD8+ T cells
903 shapes the immunodominance hierarchy during boost vaccination. *J Exp.*
904 *Med* **204**:2187-2198.
- 905 29. **Kennedy, R. and G. A. Poland.** 2007. T-Cell epitope discovery for
906 variola and vaccinia viruses. *Rev Med Virol* **17**:93-113.
- 907 30. **Kennedy, R. B., I. Ovsyannikova, and G. A. Poland.** 2009. Smallpox
908 vaccines for biodefense. *Vaccine* **27 Suppl 4**:D73-D79.
- 909 31. **Kennedy, R. B., I. G. Ovsyannikova, R. M. Jacobson, and G. A.**
910 **Poland.** 2009. The immunology of smallpox vaccines. *Curr. Opin.*
911 *Immunol.* **21**:314-320.
- 912 32. **Kondo, E., Y. Akatsuka, K. Kuzushima, K. Tsujimura, S. Asakura, K.**
913 **Tajima, Y. Kagami, Y. Koder, M. Tanimoto, Y. Morishima, and T.**
914 **Takahashi.** 2004. Identification of novel CTL epitopes of CMV-pp65
915 presented by a variety of HLA alleles. *Blood* **103**:630-638.
- 916 33. **Kozlowski, S., M. Corr, M. Shirai, L. F. Boyd, C. D. Pendleton, J. A.**
917 **Berzofsky, and D. H. Margulies.** 1993. Multiple pathways are involved
918 in the extracellular processing of MHC class-I-restricted peptides. *J.*
919 *Immunol.* **151**:4033-4044.
- 920 34. **Lafuente, E. M. and P. A. Reche.** 2009. Prediction of MHC-peptide
921 binding: a systematic and comprehensive overview. *Curr. Pharm. Des*
922 **15**:3209-3220.

- 923 35. **Larsen, M. V., M. Nielsen, A. Weinzierl, and L. O.** 2006. TAP-
924 Independent MHC Class I Presentation. *Current Immunology Reviews*
925 **2**:233-245.
- 926 36. **Lautscham, G., S. Mayrhofer, G. Taylor, T. Haigh, A. Leese, A.**
927 **Rickinson, and N. Blake.** 2001. Processing of a multiple membrane
928 spanning Epstein-Barr virus protein for CD8⁺ T cell recognition reveals a
929 proteasome-dependent, transporter associated with antigen processing-
930 independent pathway. *J. Exp. Med.* **194**:1053-1068.
- 931 37. **Lautscham, G., A. Rickinson, and N. Blake.** 2003. TAP-independent
932 antigen presentation on MHC class I molecules: lessons from Epstein-
933 Barr virus. *Microbes. Infect.* **5**:291-299.
- 934 38. **Lippincott-Schwartz, J., J. G. Donaldson, A. Schweizer, E. G.**
935 **Berger, H. P. Hauri, L. C. Yuan, and R. D. Klausner.** 1990.
936 Microtubule-dependent retrograde transport of proteins into the ER in the
937 presence of brefeldin A suggests an ER recycling pathway. *Cell* **60**:821-
938 836.
- 939 39. **López, D., B. C. Gil-Torregrosa, C. Bergmann, and M. Del Val.** 2000.
940 Sequential cleavage by metallopeptidases and proteasomes is involved
941 in processing HIV-1 ENV epitope for endogenous MHC class I antigen
942 presentation. *J. Immunol.* **164**:5070-5077.
- 943 40. **López, D., Y. Samino, U. H. Koszinowski, and M. Del Val.** 2001. HIV
944 envelope protein inhibits MHC class I presentation of a cytomegalovirus
945 protective epitope. *J. Immunol.* **167**:4238-4244.
- 946 41. **Lorente, E., R. Garcia, and D. Lopez.** 2011. Allele-dependent
947 processing pathways generate the endogenous human leukocyte antigen
948 (HLA) class I peptide repertoire in TAP-deficient cells. *J Biol. Chem.*
- 949 42. **Lorente, E., S. Infantes, E. Barnea, I. Beer, R. Garcia, F. Lasala, M.**
950 **Jimenez, A. Admon, and D. López.** 2011. TAP-independent human
951 histocompatibility complex-Cw1 antigen processing of an HIV envelope
952 protein conserved peptide. *AIDS* **25**:265-269.
- 953 43. **Lundegaard, C., O. Lund, S. Buus, and M. Nielsen.** 2010. Major
954 histocompatibility complex class I binding predictions as a tool in epitope
955 discovery. *Immunology* **130**:309-318.
- 956 44. **Medina, F., M. Ramos, S. Iborra, P. de León, M. Rodríguez-Castro,**
957 **and M. Del Val.** 2009. Furin-processed antigens targeted to the
958 secretory route elicit functional TAP1^{-/-} CD8⁺ T lymphocytes *in vivo*. *J.*
959 *Immunol.* **183**:4639-4647.
- 960 45. **Meyer, V. S., W. Kastenmuller, G. Gasteiger, M. Franz-Wachtel, T.**
961 **Lamkemeyer, H. G. Rammensee, S. Stevanovic, D. Sigurdardottir,**
962 **and I. Drexler.** 2008. Long-term immunity against actual poxviral HLA
963 ligands as identified by differential stable isotope labeling. *J Immunol.*
964 **181**:6371-6383.

- 965 46. **Moss, B.** 1991. Vaccinia virus: a tool for research and vaccine
966 development. *Science* **252**:1662-1667.
- 967 47. **Nuchtern, J. G., J. S. Bonifacino, W. E. Biddison, and R. D.**
968 **Klausner.** 1989. Brefeldin A implicates egress from endoplasmic
969 reticulum in class I restricted antigen presentation. *Nature* **339**:223-226.
- 970 48. **Omura, S., T. Fujimoto, K. Otaguro, K. Matsuzaki, R. Moriguchi, H.**
971 **Tanaka, and Y. Sasaki.** 1991. Lactacystin, a novel microbial metabolite,
972 induces neuritogenesis of neuroblastoma cells. *J. Antibiot. (Tokyo)*
973 **44**:113-116.
- 974 49. **Oseroff, C., F. Kos, H. H. Bui, B. Peters, V. Pasquetto, J. Glenn, T.**
975 **Palmore, J. Sidney, D. C. Tscharke, J. R. Bennink, S. Southwood, H.**
976 **M. Grey, J. W. Yewdell, and A. Sette.** 2005. HLA class I-restricted
977 responses to vaccinia recognize a broad array of proteins mainly
978 involved in virulence and viral gene regulation. *Proc. Natl. Acad. Sci. U.*
979 *S. A* **102**:13980-13985.
- 980 50. **Parham, P. and W. F. Bodmer.** 1978. Monoclonal antibody to a human
981 histocompatibility alloantigen, HLA-A2. *Nature* **276**:397-399.
- 982 51. **Pascolo, S., N. Bervas, J. M. Ure, A. G. Smith, F. A. Lemonnier, and**
983 **B. Perarnau.** 1997. HLA-A2.1-restricted education and cytolytic activity
984 of CD8(+) T lymphocytes from beta2 microglobulin (beta2m) HLA-A2.1
985 monochain transgenic H-2Db beta2m double knockout mice. *J Exp. Med.*
986 **185**:2043-2051.
- 987 52. **Pasquetto, V., H. H. Bui, R. Giannino, F. Mirza, J. Sidney, C. Oseroff,**
988 **D. C. Tscharke, K. Irvine, J. R. Bennink, B. Peters, S. Southwood, V.**
989 **Cerundolo, H. Grey, J. W. Yewdell, and A. Sette.** 2005. HLA-A*0201,
990 HLA-A*1101, and HLA-B*0702 transgenic mice recognize numerous
991 poxvirus determinants from a wide variety of viral gene products. *J.*
992 *Immunol.* **175**:5504-5515.
- 993 53. **Rammensee, H. G., J. Bachmann, N. P. N. Emmerich, O. A. Bachor,**
994 **and S. Stevanovic.** 1999. SYFPEITHI: database for MHC ligands and
995 peptide motifs. *Immunogenetics* **50**:213-219.
- 996 54. **Rawlings, N. D. and A. J. Barrett.** 1995. Evolutionary families of
997 metallopeptidases, p. 183-229. *Methods in Enzymology.* Barrett, A.J.
998 (ed), Academic Press, New York.
- 999 55. **Redfield, R. R., D. C. Wright, W. D. James, T. S. Jones, C. Brown,**
1000 **and D. S. Burke.** 1987. Disseminated vaccinia in a military recruit with
1001 human immunodeficiency virus (HIV) disease. *N. Engl. J. Med.* **316**:673-
1002 676.
- 1003 56. **Rico, M. A., A. Trento, M. Ramos, C. Johnstone, M. Del Val, J. A.**
1004 **Melero, and D. López.** 2009. Human respiratory syncytial virus infects
1005 and induces activation markers in mouse B lymphocytes. *Immunol. Cell*
1006 *Biol.* **87**:344-350.

- 1007 57. **Salter, R. D. and P. Cresswell.** 1986. Impaired assembly and transport
1008 of HLA-A and -B antigens in a mutant TxB cell hybrid. *EMBO J.* **5**:943-
1009 949.
- 1010 58. **Samino, Y., D. López, S. Guil, P. de León, and M. Del Val.** 2004. An
1011 endogenous HIV envelope-derived peptide without the terminal NH₃⁺
1012 group is physiologically presented by major histocompatibility class I
1013 molecules. *J. Biol. Chem.* **279**:1151-1160.
- 1014 59. **Saric, T., S. C. Chang, A. Hattori, I. A. York, S. Markant, K. L. Rock,**
1015 **M. Tsujimoto, and A. L. Goldberg.** 2002. An IFN- γ -induced
1016 aminopeptidase in the ER, ERAP1, trims precursors to MHC class I-
1017 presented peptides. *Nat. Immunol.* **3**:1169-1176.
- 1018 60. **Schramm, B. and J. K. Locker.** 2005. Cytoplasmic organization of
1019 POXvirus DNA replication. *Traffic.* **6**:839-846.
- 1020 61. **Serwold, T., F. González, J. Kim, R. Jacob, and N. Shastri.** 2002.
1021 ERAAP customizes peptides for MHC class I molecules in the
1022 endoplasmic reticulum. *Nature* **419**:480-483.
- 1023 62. **Slee, E. A., H. Zhu, S. C. Chow, M. MacFarlane, D. W. Nicholson, and**
1024 **G. M. Cohen.** 1996. Benzyloxycarbonyl-Val-Ala-Asp (OMe)
1025 fluoromethylketone (Z- VAD.FMK) inhibits apoptosis by blocking the
1026 processing of CPP32. *Biochem. J.* **315**:21-24.
- 1027 63. **Spies, T. and R. DeMars.** 1991. Restored expression of major
1028 histocompatibility class I molecules by gene transfer of a putative peptide
1029 transporter. *Nature* **351**:323-324.
- 1030 64. **Thornberry, N. A.** 1994. Interleukin-1 beta converting enzyme. *Methods*
1031 *Enzymol.* **244:615-31**:615-631.
- 1032 65. **Umezawa, H.** 1976. Structures and activities of protease inhibitors of
1033 microbial origin. *Methods Enzymol.* **45**:678-695.
- 1034 66. **Villadangos, J. A., B. Galocha, and J. A. Lopez de Castro.** 1994.
1035 Unusual topology of an HLA-B27 allospecific T cell epitope lacking
1036 peptide specificity. *J. Immunol.* **152**:2317-2323.
- 1037 67. **Wang, M., K. Lamberth, M. Harndahl, G. Roder, A. Stryhn, M. V.**
1038 **Larsen, M. Nielsen, C. Lundegaard, S. T. Tang, M. H. Dziegiel, J.**
1039 **Rosenkvist, A. E. Pedersen, S. Buus, M. H. Claesson, and O. Lund.**
1040 2007. CTL epitopes for influenza A including the H5N1 bird flu; genome-,
1041 pathogen-, and HLA-wide screening. *Vaccine* **25**:2823-2831.
- 1042 68. **Weihofen, A., K. Binns, M. K. Lemberg, K. Ashman, and B.**
1043 **Martoglio.** 2002. Identification of signal peptide peptidase, a presenilin-
1044 type aspartic protease. *Science* **296**:2215-2218.
- 1045 69. **Weihofen, A., M. K. Lemberg, H. L. Ploegh, M. Bogyo, and B.**
1046 **Martoglio.** 2000. Release of signal peptide fragments into the cytosol

- 1047 requires cleavage in the transmembrane region by a protease activity
1048 that is specifically blocked by a novel cysteine protease inhibitor. *J. Biol.*
1049 *Chem.* **275**:30951-30956.
- 1050 70. **Weinzierl, A. O., D. Rudolf, N. Hillen, S. Tenzer, P. van Endert, H.**
1051 **Schild, H. G. Rammensee, and S. Stevanovic.** 2008. Features of TAP-
1052 independent MHC class I ligands revealed by quantitative mass
1053 spectrometry. *Eur J Immunol.*
- 1054 71. **Yewdell, J. W. and J. R. Bennink.** 1989. Brefeldin A specifically inhibits
1055 presentation of protein antigens to cytotoxic T lymphocytes. *Science*
1056 **244**:1072-1075.
- 1057 72. **York, I. A., S. C. Chang, T. Saric, J. A. Keys, J. M. Favreau, A. L.**
1058 **Goldberg, and K. L. Rock.** 2002. The ER aminopeptidase ERAP1
1059 enhances or limits antigen presentation by trimming epitopes to 8-9
1060 residues. *Nat. Immunol.* **3**:1177-1184.
- 1061 73. **York, I. A., A. L. Goldberg, X. Y. Mo, and K. L. Rock.** 1999. Proteolysis
1062 and class I major histocompatibility complex antigen presentation.
1063 *Immunol. Rev.* **172**:49-66.
1064
1065

Table 1
Specificity and activity of the inhibitors used in this study

Inhibitor	Abbreviation	Specificity	Reference	Concentration	% Inhibition of degradation ^a
Brefeldin A	BFA	Vesicle transport	(71)(47)	5 µg/ml	ND
Lactacystin	LC	Proteasome	(18)(48)	10 µM	ND
(z-LL) ₂ ketone	z-LL ₂	Signal peptide peptidase	(69)(68)	100 µM	13 ± 4
Leupeptin	LEU	Trypsin-like proteases and cysteine proteases	(65)	100 µM	38 ± 18
Pepstatin	PEPST	Aspartic proteases	(33)(65)	100 µM	50 ± 5
1-10 Phenanthroline	PHE	Metalloproteases and caspase-1	(33)(64)	50 µM	ND
Leucinethiol	LeuSH	Metallo-aminopeptidases including ERAAP	(61)	30 µM	ND
Benzyl Succinyl Acid	BENZ	Metallo-carboxypeptidases A & B	(33)	100µM	-10 ± 8
Captopril	CAPT	ACE and ACE-like proteases	(33)	100 µM	25 ± 2
Phosphoramidon	PHOSP	All bacterial metallo-endopeptidases but few of mammalian origin	(21)(33)	100 µM	15 ± 4
z-VAD.fmk	z-VAD	Caspases	(62)	100 µM	ND ^b

^a Activity of these inhibitors was measured as their ability to prevent proteolytic degradation in cellular extracts as in reference (39). The amount of protein still present after incubation in the case of the degraded control sample was considered as 0 % inhibition of degradation, and the non-degraded unincubated sample was taken as 100 % inhibition. Data are mean of two independent experiments. Negative values indicate that there was enhanced degradation in the presence of the compound. ND, not done.

^b The compound was found to block apoptosis (data not shown).

Table 2

Summary of HLA molecules bound by vaccinia virus epitopes

Ligand	Sequence	mAb used ^a	HLA-A2	HLA-B27	HLA-B51	HLA-Cw1
A17L ₉₋₁₇	MLDDFSAGA	PA2.1	+ ^b	ND	ND	ND
A10L ₆₁₄₋₆₂₃	SPEGEETII	PA2.1	+	ND	ND	ND
A10L ₆₈₈₋₆₉₆	ILDRIITNA	PA2.1	+	ND	ND	ND
A10L ₈₆₇₋₈₇₆	SRGYFEHMKK	ME1	ND ^c	+	ND	ND
B8R ₅₃₋₅₉	WQTMYYTN	ME1	ND	+	ND	ND
K2L ₁₆₋₃₀	YRLQGFTNAGIVAYK	ME1 / W6-32	-	+	-	+
D5R ₁₄₈₋₁₅₇	IAMKRTLLEL	W6-32	-	ND	+	-
A50R ₂₉₄₋₃₀₁	LPFGSLGI	W6-32	-	ND	+	-
C11R ₁₀₁₋₁₁₀	IPSPGIMLV	W6-32	-	ND	+	+
A17L ₉₋₂₅	MLDDFSAGAGVLDKDL	W6-32	-	ND	-	+
D8L ₁₁₂₋₁₁₉	DGLIISI	W6-32	-	ND	-	+

^a The mAbs used for the sequential immunoprecipitations were PA2.1 (specific for HLA-A2), ME1 (specific for HLA-B27), and W6/32 (specific for a monomorphic HLA-A, B, C determinant).

^b A significant difference ($P < 0.001$) compared with the negative controls.

^c ND, not done.

Table 3

Conservation of viral HLA ligands in several orthopoxviruses

Poxvirus ^a	A17L ₉₋₁₇ (HLA-A2)	A10L ₆₁₄₋₆₂₃ (HLA-A2)	A10L ₆₈₈₋₆₉₆ (HLA-A2)	A10L ₈₆₇₋₈₇₆ (HLA-B27)	B8R ₅₃₋₅₉ (HLA-B27)	K2L ₁₆₋₃₀ (HLA-B27, -Cw1)
VACV WR	MLDDFSAGA	SPEGEETII	ILDRIITNA	SRGYFEHMKK	WQTMYSN	YRLQGFTNAGIVAYK
VACV Copenhagen	-----	-----	-----	-----	-----	-----
VACV MVA	-----	-----	-----	-----	-----	-----
Variola major	-----	-----	-----	-----	-----	-----
Variola minor	-----	-----	-----	-----	-----	-----
Camelpox	-----	-----	-----	-----	-----	-----
Cowpox	-----	-----	-----	-----	-----	-----
Ectromelia virus	-----	-----	-----	-----	-----	-----
Horsepox	-----	-----	-----	-----	-----	-----
Monkeypox	-----	-----	-----	-----	-----	-----
Rabbitpox	-----	-----	-----	-----	-----	-----
Taterapox	-----	-----	-----	-----	-----	-----

Poxvirus ^a	D5R ₁₄₈₋₁₅₇ (HLA-B51)	A50R ₂₉₄₋₃₀₁ (HLA-B51)	C11R ₁₀₁₋₁₁₀ (HLA-B51, -Cw1)	A17L ₉₋₂₅ (HLA-Cw1)	D8L ₁₁₂₋₁₁₉ (HLA-Cw1)
VACV WR	IAMKRTLLEL	LPGFSLGI	IPSPGIMLV	MLDDFSAGAGVLDKDL	DGLIIISI
VACV Copenhagen	-----	-----	-----	-----	-----
VACV MVA	-----	-----	-----	-----	-----
Variola major	-----	-----	-----V--	-----	-----
Variola minor	-----	-----	-----V--	-----	-----
Camelpox	-----	-----	-----V--	-----	-----
Cowpox	-----	-----	-----V--	-----	--I--VA-
Ectromelia virus	-----	-----	-----	-----	-----
Horsepox	-----	-----	-----	-----	-----
Monkeypox	-----	-----	---L--V--	-----	--I--A-
Rabbitpox	-----	-----	-----V--	-----	-----
Taterapox	-----	-----	-----V--	-----	-----

^a The sequences used were obtained from the NCBI database (<http://blast.ncbi.nlm.nih.gov/Blast.cgi>).

Table 4

TAP-independent ligands/epitopes and their hydrophobicity.

Ligand/epitope	Protein	Virus	Hydrophobicity ^a	Reference
LLWTLVLL	LMP2	EBV	2.9	(37)
CLGGLLTMV	LMP2	EBV	2.1	(37)
Mean ± SD of 8 TAP ⁻ epitopes		EBV	2.5 ± 0.2	(37)
MLDDFSAGA	A17L ₉₋₁₇	Vaccinia	0.4	This study
SPEGEETII	A10L ₆₁₄₋₆₂₃	Vaccinia	-0.6	This study
ILDRIITNA	A10L ₆₈₈₋₆₉₆	Vaccinia	0.8	This study
SRGYFEHMKK	A10L ₈₆₇₋₈₇₆	Vaccinia	-1.7	This study
WQTMVTN	B8R ₅₃₋₅₉	Vaccinia	-1.2	This study
YRLQGFTNAGIVAYK	K2L ₁₆₋₃₀	Vaccinia	-0.1	This study
IAMKRTLLEL	D5R ₁₄₈₋₁₅₇	Vaccinia	0.7	This study
LPGSLGI	A50R ₂₉₄₋₃₀₁	Vaccinia	1.5	This study
IPSPGIMLV	C11R ₁₀₁₋₁₁₀	Vaccinia	1.6	This study
MLDDFSAGAGVLDKDL	A17L ₉₋₂₅	Vaccinia	0.3	This study
DGLIISI	D8L ₁₁₂₋₁₁₉	Vaccinia	2.1	This study
Mean ± SD of 11 TAP ⁻ ligands		Vaccinia	0.3 ± 1.2	This study
		P value	< 0.0001	
Mean ± SD of 79 TAP ⁺ epitopes		Vaccinia	0.4 ± 1.0	(45)(25)

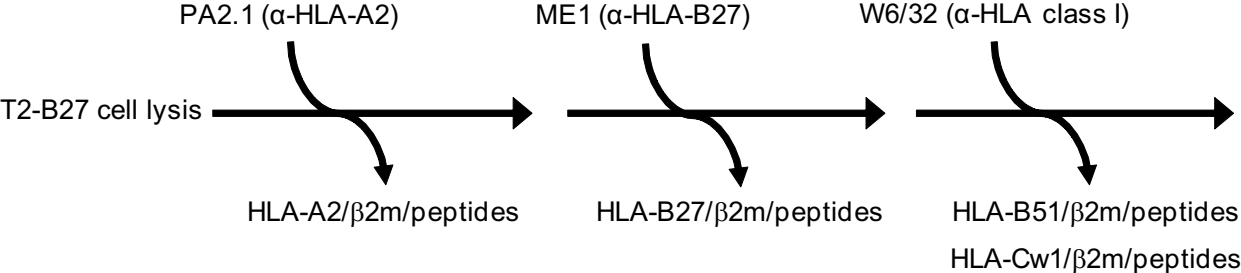
^a as measured on the grand average of hydropathicity (GRAVY) scale (ProtParam tool, ExPASy Proteomics Server, <http://www.expasy.ch>).

Table 5

Comparison between predicted and experimentally detected binding of vaccinia virus ligands to HLA molecules

Ligand	Sequence	HLA	
		Predicted ^a	Experimentally detected
A17L ₉₋₁₇	MLDDFSAGA	-A2	-A2
A10L ₆₁₄₋₆₂₃	SPEGEETII	-B51	-A2
A10L ₆₈₈₋₆₉₆	ILDRIITNA	-A2	-A2
A10L ₈₆₇₋₈₇₆	SRGYFEHMKK	-B27	-B27
B8R ₅₃₋₅₉	WQTMYPN	-B27	-B27
K2L ₁₆₋₃₀	YRLQGFTNAGIVAYK	-B27	-B27 / -Cw1
D5R ₁₄₈₋₁₅₇	IAMKRTLLEL	-B51 / -Cw1	-B51
A50R ₂₉₄₋₃₀₁	LPFGSLGI	-B51	-B51
C11R ₁₀₁₋₁₁₀	IPSPGIMLV	-B51	-B51 / -Cw1
A17L ₉₋₂₅	MLDDFSAGAGVLDKDL	-A2 / -Cw1	-Cw1
D8L ₁₁₂₋₁₁₉	DGLIIISI	-B51	-Cw1

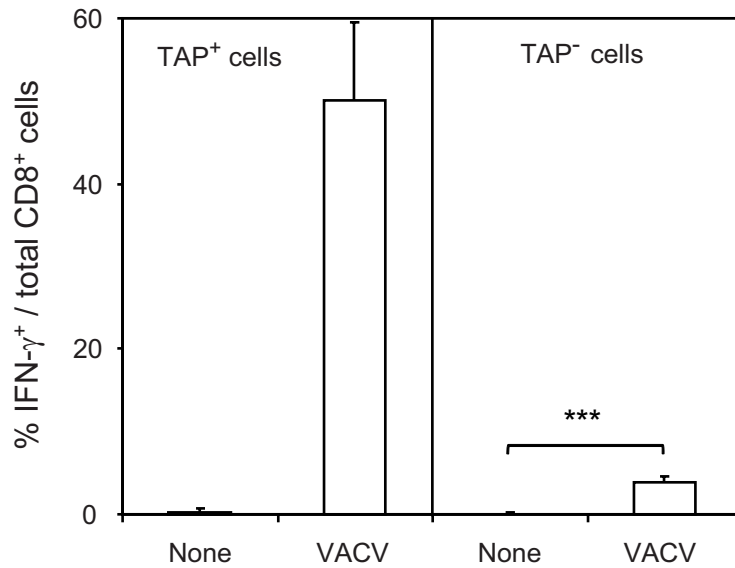
^a From the SYFPEITHI (<http://www.syfpeithi.de>), BIMAS (<http://www-bimas.cit.nih.gov>), and IEDB (<http://www.immuneepitope.org>) databases.



Lorente et al. Figure 1

Diagram of sequential immunoprecipitation.

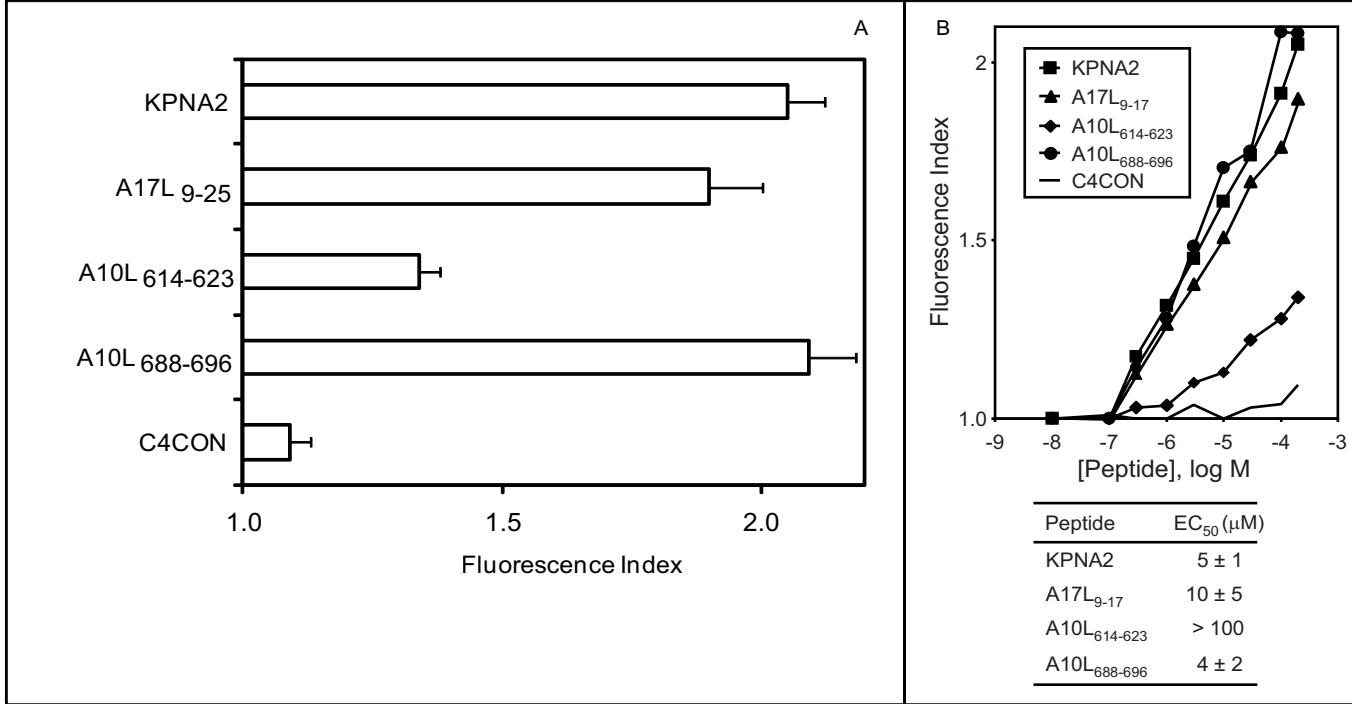
4×10^{10} healthy or VACV-infected T2-B27 transfectant cells were lysed. HLA-peptide complexes were isolated via affinity chromatography of the soluble fraction of cell extracts with the following mAbs, used sequentially: PA2.1 (anti-HLA-A2), ME1 (anti-HLA-B27), and W6/32 (specific for a monomorphic HLA class I determinant).



Lorente et al. Figure 2

Recognition of TAP⁺ and TAP⁻ cell lines by VACV-specific CD8⁺ T lymphocytes.

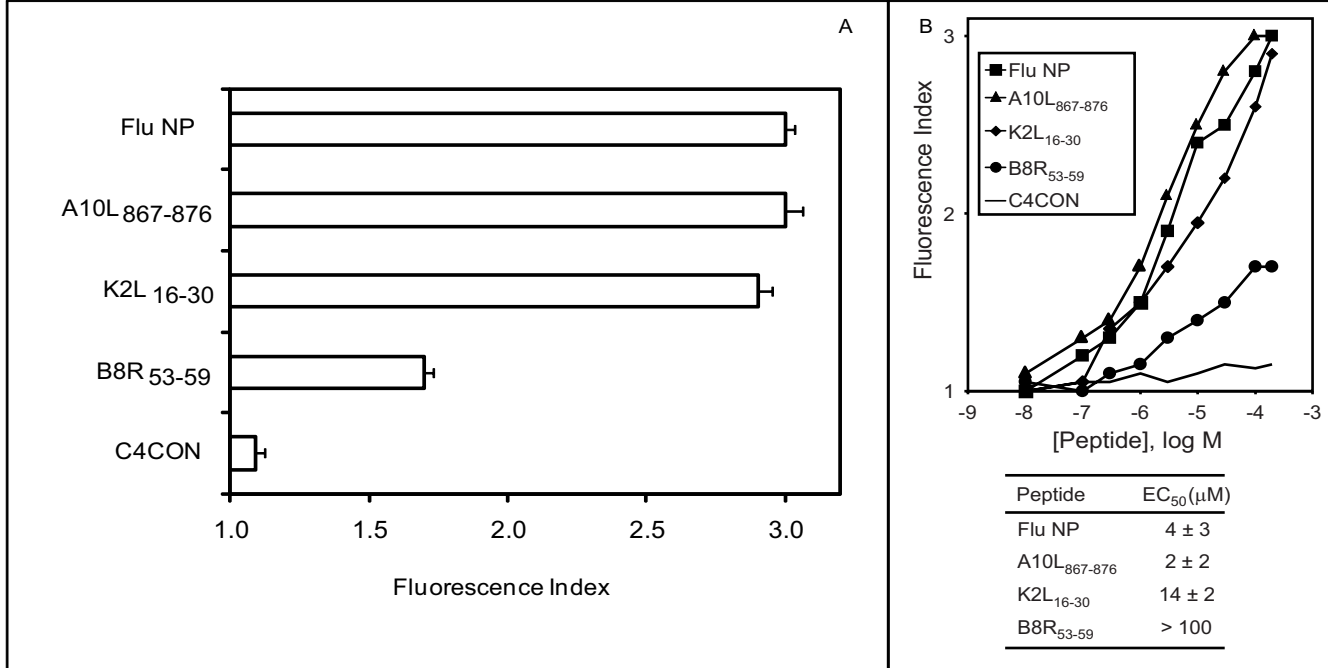
HLA-A*0201 TAP⁺ (RMA, left panel) and TAP⁻ (RMA-S, right panel) cells were infected with VACV at a multiplicity of infection of 40 plaque-forming units/cell and analyzed by ICS for CD8⁺ T cell activation. The results are calculated as the mean of three or four independent experiments \pm SD. *** Significant P values ($P < 0.0001$).



Lorente et al. Figure 3

HLA-A*0201 stabilization assay with synthetic VACV ligands.

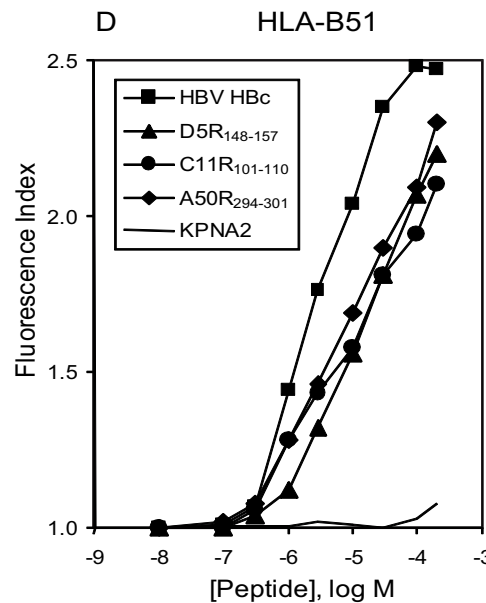
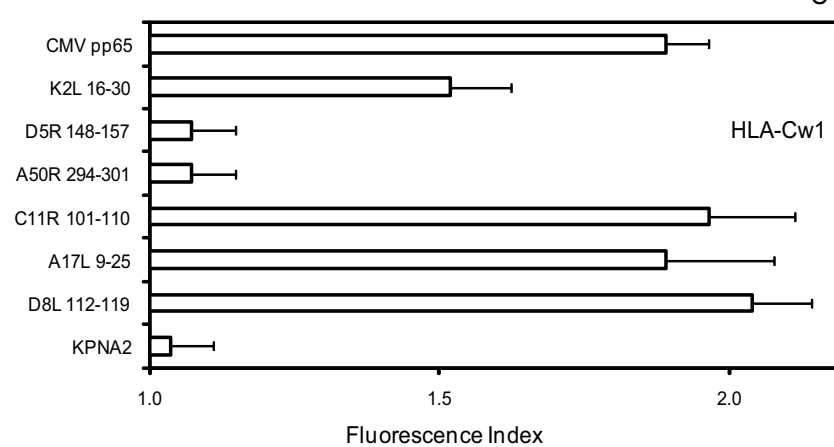
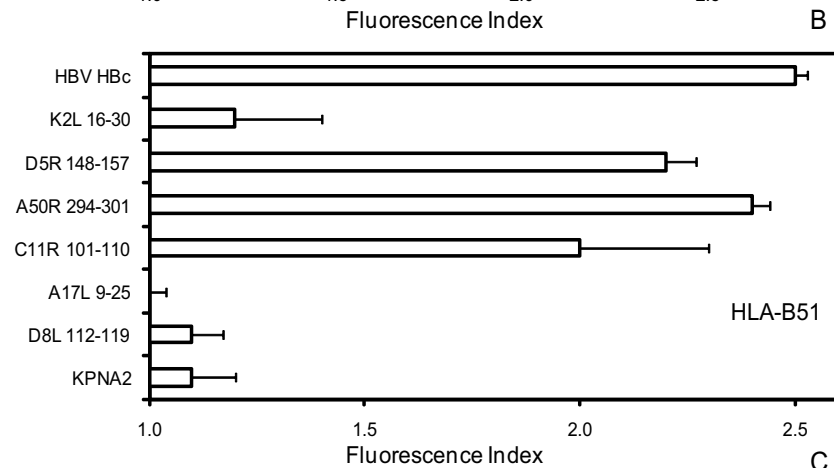
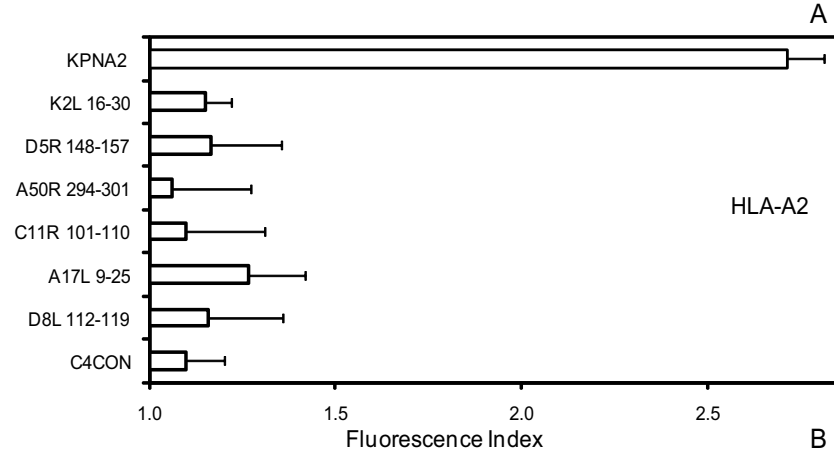
The stability of HLA-A*0201/peptide complexes on the surface of RMA-S transfectant cells was measured by flow cytometry. The indicated peptides were used at 200 μM (panel A). The mAb used was the monoclonal PA2.1. Panel B: The titration curves for synthetic VACV A17L₉₋₁₇ (triangles), A10L₆₁₄₋₆₂₃ (diamonds), and A10L₆₈₈₋₆₉₆ (circles) peptides with HLA-A*0201 are depicted. The C4CON (solid line) and KPNA2 (squares) peptides were used as negative and positive controls, respectively. The results, calculated as the fluorescence index (panel A), are the mean of three or four independent experiments. The calculated EC₅₀ values ± SD are shown in panel B.



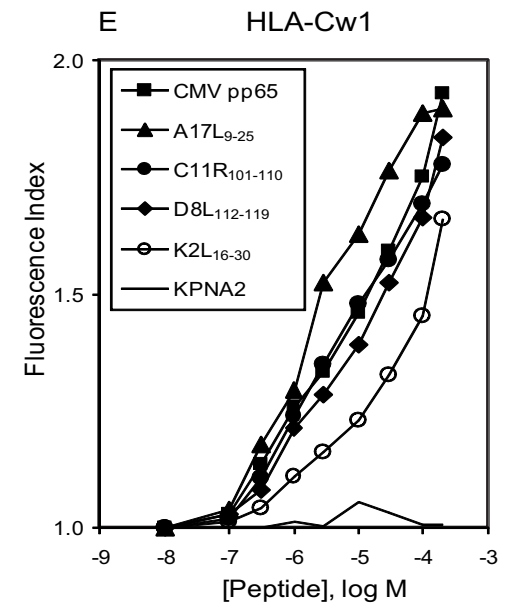
Lorente et al. Figure 4

HLA-B*2705 stabilization assay with synthetic VACV ligands.

The stability of HLA-B*2705/peptide complexes on the surface of RMA-S transfectant cells measured by flow cytometry. The indicated peptides were used at 200 μM (panel A). The mAb used was the monoclonal ME1. Panel B: The titration curves for synthetic VACV A10L₈₆₇₋₈₇₆ (triangles), K2L₁₆₋₃₀ (diamonds), and B8R₅₃₋₅₉ (circles) peptides with HLA- B*2705 are depicted. The C4CON (solid line) and Flu NP (squares) peptides were used as negative and positive controls, respectively. The results, as in Figure 2, are the mean of four independent experiments.



Peptide	EC ₅₀ (μ M)
HBV HBc	2 \pm 1
D5R ₁₄₈₋₁₅₇	19 \pm 6
C11R ₁₀₁₋₁₁₀	18 \pm 11
A50R ₂₉₄₋₃₀₁	22 \pm 7

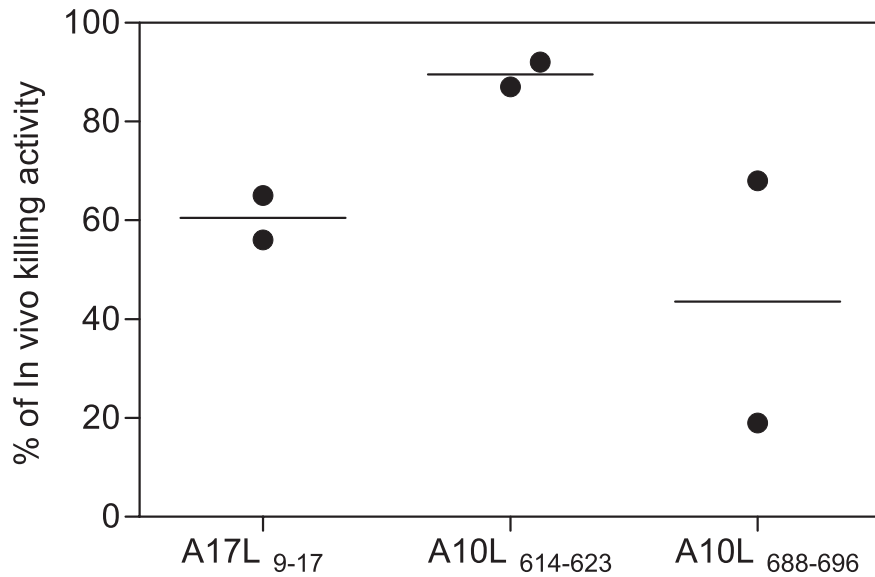


Peptide	EC ₅₀ (μ M)
CMV pp65	12 \pm 4
A17L ₉₋₂₅	2 \pm 1
C11R ₁₀₁₋₁₁₀	7 \pm 4
D8L ₁₁₂₋₁₁₉	18 \pm 7
K2L ₁₆₋₃₀	70 \pm 10

Lorente et al. Figure 5

HLA class I stabilization assay of synthetic VACV ligands.

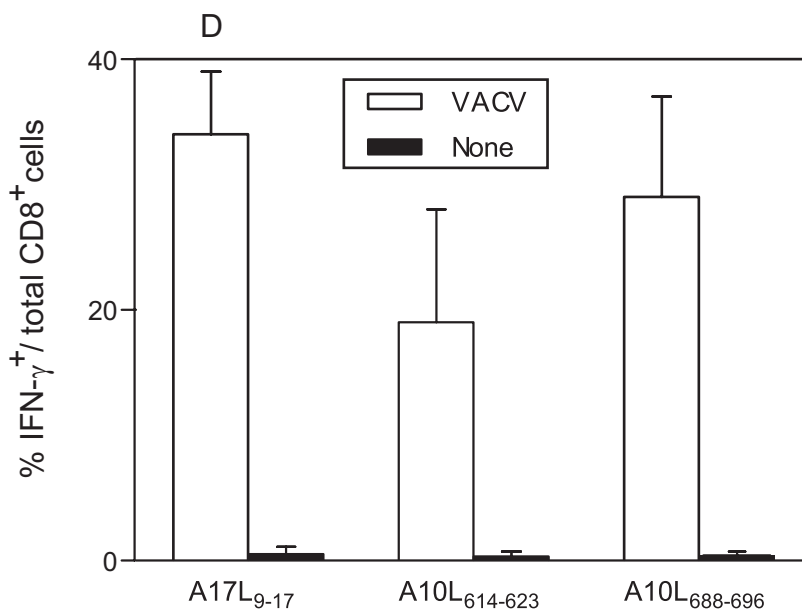
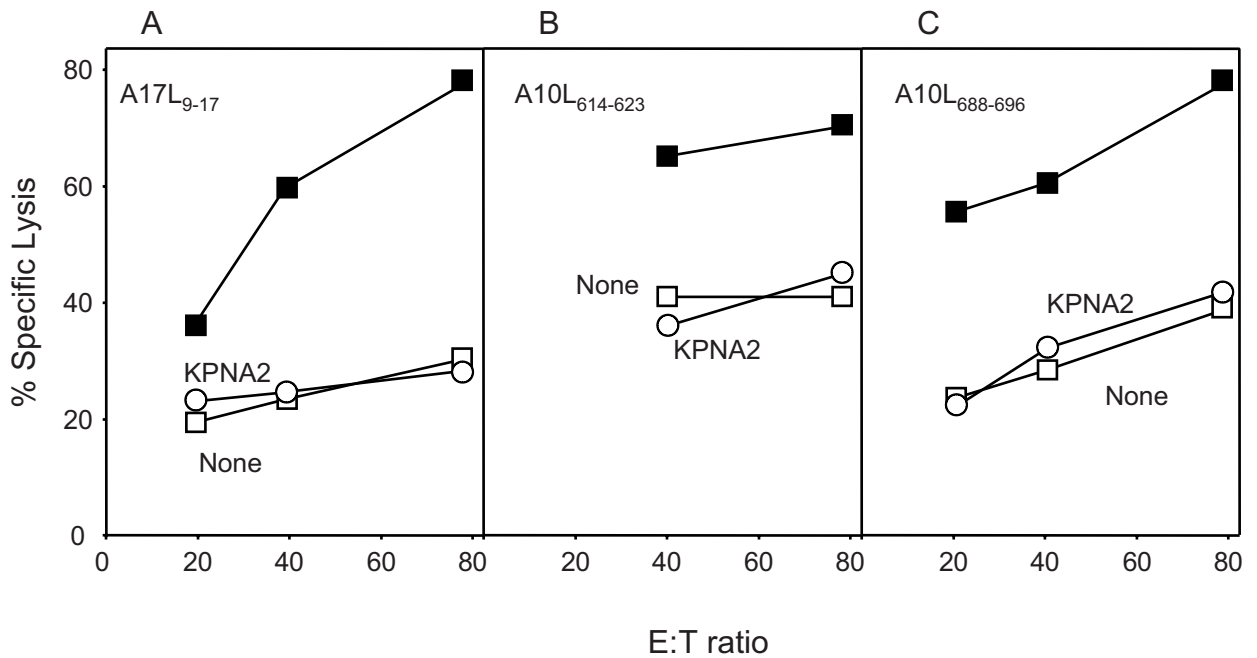
The stability of HLA-A2 (panel A), -B51 (panel B), and -Cw1 (panel C) at the cell surface of T2 TAP-deficient cells was measured by flow cytometry. The indicated peptides were used at 200 μ M. Titration curves for the indicated synthetic VACV peptides, immunoprecipitated with W6/32 Ab, with HLA-B51 (panel D) or -Cw1 (panel E) are shown. The C4CON peptide was used as negative control (solid line). The HBV HBC₁₉₋₂₇ and CMV pp65₇₋₁₅ peptides were used as positive controls for binding to the HLA-B51 and -Cw1 alleles, respectively. The Abs used were monoclonal PA2.1 (anti-HLA-A2, panel A), polyclonal H00003106-B01P (anti-HLA-B class I molecules, panel B, D), and polyclonal SC-19438 (anti-HLA-C class I molecules, panel C, E). The results, as in Figure 2, are the mean of four to six independent experiments.



Lorente et al Figure 6

In vivo killing activity of VACV peptide-specific CTLs in HLA-A*0201-transgenic mice.

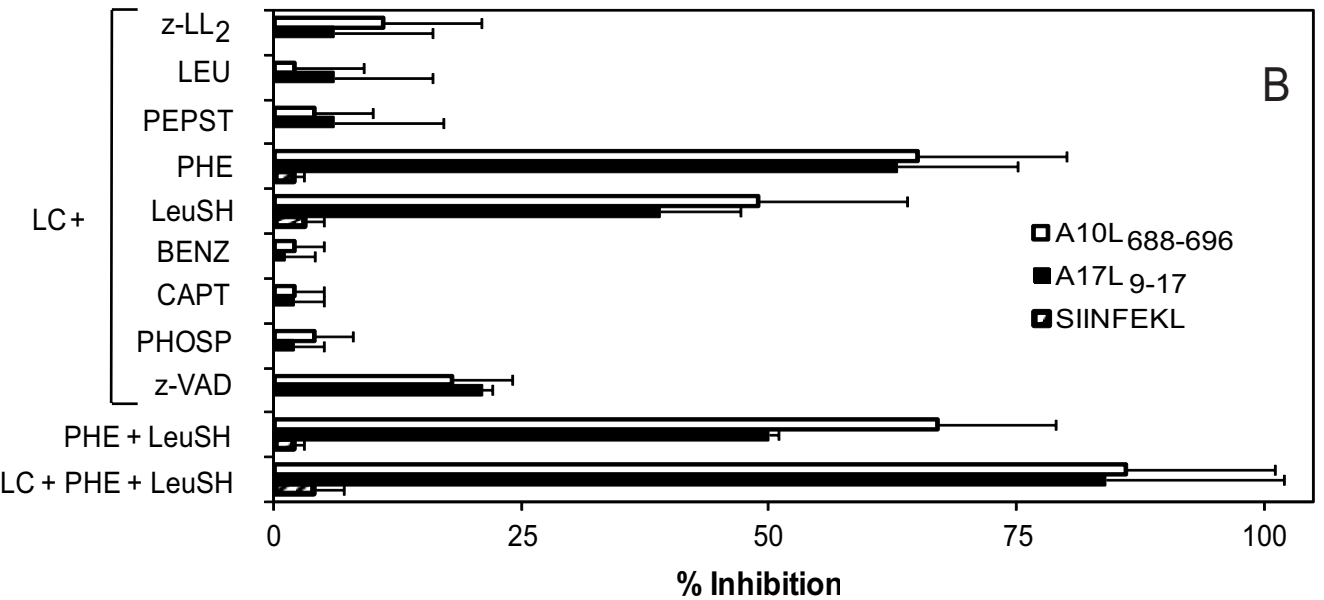
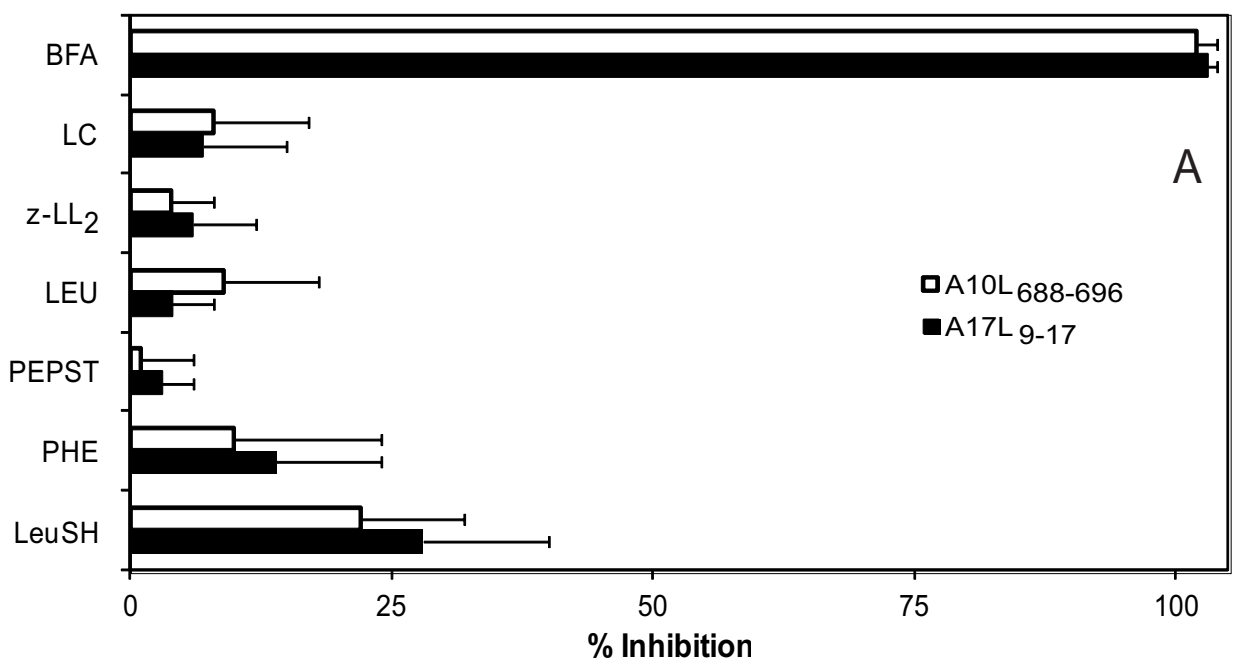
HLA-A*0201-transgenic mice were infected i.p. with VAVC. One week later, they were injected i.p. with syngeneic splenocytes either unpulsed and labeled with low CFSE (none) or pulsed with the indicated VACV peptides and labeled with high CFSE. Two days later, remaining CFSE-labeled target cells in the peritoneal cavity were lavaged and analyzed by flow cytometry. Percent in vivo lysis values of individual animals (circles) \pm SD (line) are shown.



Lorente et al. Figure 7

Recognition of VACV epitopes presented by the HLA-A*0201 class I molecule by CTLs.

RMA-HLA-A*0201 target cells pre-pulsed with 10^{-5} M A17L₉₋₁₇ (panel A), A10L₆₁₄₋₆₂₃ (panel B), and A10L₆₈₈₋₆₉₆ (panel C) synthetic peptides were tested in a cytolytic assay with their respective memory peptide-specific CTL lines obtained from HLA-A*0201-transgenic mice immunized up to 30 days before with VACV (upper panel). The KPNA2 peptide was used as negative control (open circles). The data are the mean of at least three independent experiments. HLA-A*0201 TAP⁺ cells were infected with VACV at a multiplicity of infection of 40 plaque-forming units/cell and analyzed by ICS for CD8⁺ T cell activation with the HLA-A*0201 memory peptide-specific CTL lines (lower panel). The data are the mean of 4-6 independent experiments.



Panel C: Sequence alignment of neighboring residues to the epitopes in A10L and A17L proteins. The sequence of each epitope is boxed. Identical residues in both sequences are bolded.

```

681 FCAMPYN ILDRITNA GTCTVSIGDMLDNI 710
1 MSYLRYYN MLDDFSAGA GVLDKDLFTTEEQQ 30

```

Lorente et al. Figure 8

Recognition of target cells infected in the presence of inhibitors.

RMA-HLA-A*0201 target cells infected for 16 hr with VACV or VACV-OVA₂₅₇₋₂₆₄ at a multiplicity of infection of 40 plaque-forming units/cell were treated with the indicated inhibitors. An ICS assay was used to test for recognition by A10L₆₈₈₋₆₉₆- (open bars), A17L₉₋₁₇- (closed bars) or SIINFEKL-specific (hatched bars) CTLs. The percentage of specific inhibition obtained by the addition of the indicated single (panel A) or mixture of two or three (panel B) inhibitors was calculated as:

$$\% \text{ Specific Inhibition} = 100 - \frac{[(\text{ICS VACV} + \text{Inhibitor}) - \text{ICS without infection}]}{\text{ICS VACV} - \text{ICS without infection}} \times 100$$

and the data displayed is the mean ± SD of 4-6 independent experiments. Panel C: the sequence of the neighboring residues to the epitopes in A10L and A17L proteins. The sequence of each epitope is boxed. Identical residues in both sequences are bolded.

Supplemental Table 1

Major characteristics of HLA ligand-containing vaccinia proteins ^a

Protein	Name	Expression	Signal sequence	Transmembrane domains	Encapsidated	pI	Mw	PTM ^b	Essential to VACV
A10L	P4a precursor	Late	None	0	Yes, in core	6.1	102		NI ^c
A17L	IMV membrane protein	Late	Putative	4	Yes, in membrane	4.4	23	Phosphorylation	Yes
A50R	DNA ligase	Early	None	0	No	7.9	63		No
B8R	IFN-gamma receptor	Early	Putative	0	No	5.5	31		NI
C11R	EGF growth factor	Early	Putative	1	No	6.4	16		NI
D5R	NTPase	Early	None	0	No	6.8	90		Yes
D8L	Carbonic anhydrase	Late	None	1	Yes, in membrane	8.8	35		NI
K2L	Serpin 1,2,3	Early/Late	Putative	0	No	9.0	42		NI

^a All information was obtained from the Poxvirus Bioinformatics Resources Center (<http://www.poxvirus.org>).

^b PTM, post-translational modification.

^c NI, no information.

1 **SUPPLEMENTAL FIGURE LEGENDS**

2
3 **Figure S1. VACV infection of the RMA-HLA-A*0201 cell line in presence of**
4 **different protease inhibitors.**

5
6 RMA-HLA-A*0201 target cells infected for 16 hr with VACV at a multiplicity of infection
7 of 40 plaque-forming units/cell were treated with the indicated inhibitors. A mock
8 infected control was included as negative control. The cells were stained with the
9 Omnitope antiserum-FITC that recognizes VACV purified virions. Samples were
10 analyzed by FACS. The results, calculated as fluorescence index \pm SD, are the mean
11 of 4 independent experiments. The fluorescence index was calculated as the ratio of
12 mean channel fluorescence of the sample to that of the control incubated without
13 VACV. All VACV-infected conditions (with and without inhibitors) show significant P
14 values ($P < 0.01$) versus mock infected controls. In contrast, all inhibitor conditions
15 show non significant P values versus VACV-infected control without an inhibitor.

16
17 **Figure S2. Identification of three HLA-A*0201 ligands in infected cell extracts by**
18 **mass spectrometry.**

19
20 MS/MS fragmentation spectra obtained from quadrupole ion trap mass spectrometry of
21 the ion peaks at m/z 926.4 (upper left panel), m/z 974.6 (medium left panel), and m/z
22 514.8 (lower left panel) from the VACV-infected cell extract and the corresponding
23 synthetic peptide (right panels). The vertical axis represents the relative abundance of
24 the parental ion and each fragmentation ion detected. The horizontal axis corresponds
25 to the m/z region in which significant daughter ions were detected. Ions generated by
26 the fragmentation are detailed, and the sequence deduced from the indicated
27 fragments is shown in the upper left box of each panel.

29 **Figure S3. Identification of three HLA-B27 ligands in infected cell extracts by**
30 **mass spectrometry.**

31

32 MS/MS fragmentation spectra obtained from quadrupole ion trap mass spectrometry of
33 the ion peaks at m/z 428.2 (upper left panel), m/z 567.6 (medium left panel), and m/z
34 472.1 (lower left panel) from the VACV-infected cell extract and the corresponding
35 synthetic peptide (right panels). The axes are as described in Figure S1.

36

37 **Figure S4. Identification of three HLA ligands in infected cell extracts by mass**
38 **spectrometry (I).**

39

40 MS/MS fragmentation spectra obtained from quadrupole ion trap mass spectrometry of
41 the ion peaks at m/z 594.4 (upper left panel), m/z 803.5 (medium left panel), and m/z
42 926.5 (lower left panel) from the VACV-infected cell extract and the corresponding
43 synthetic peptide (right panels). The axes are as described in Figure S1.

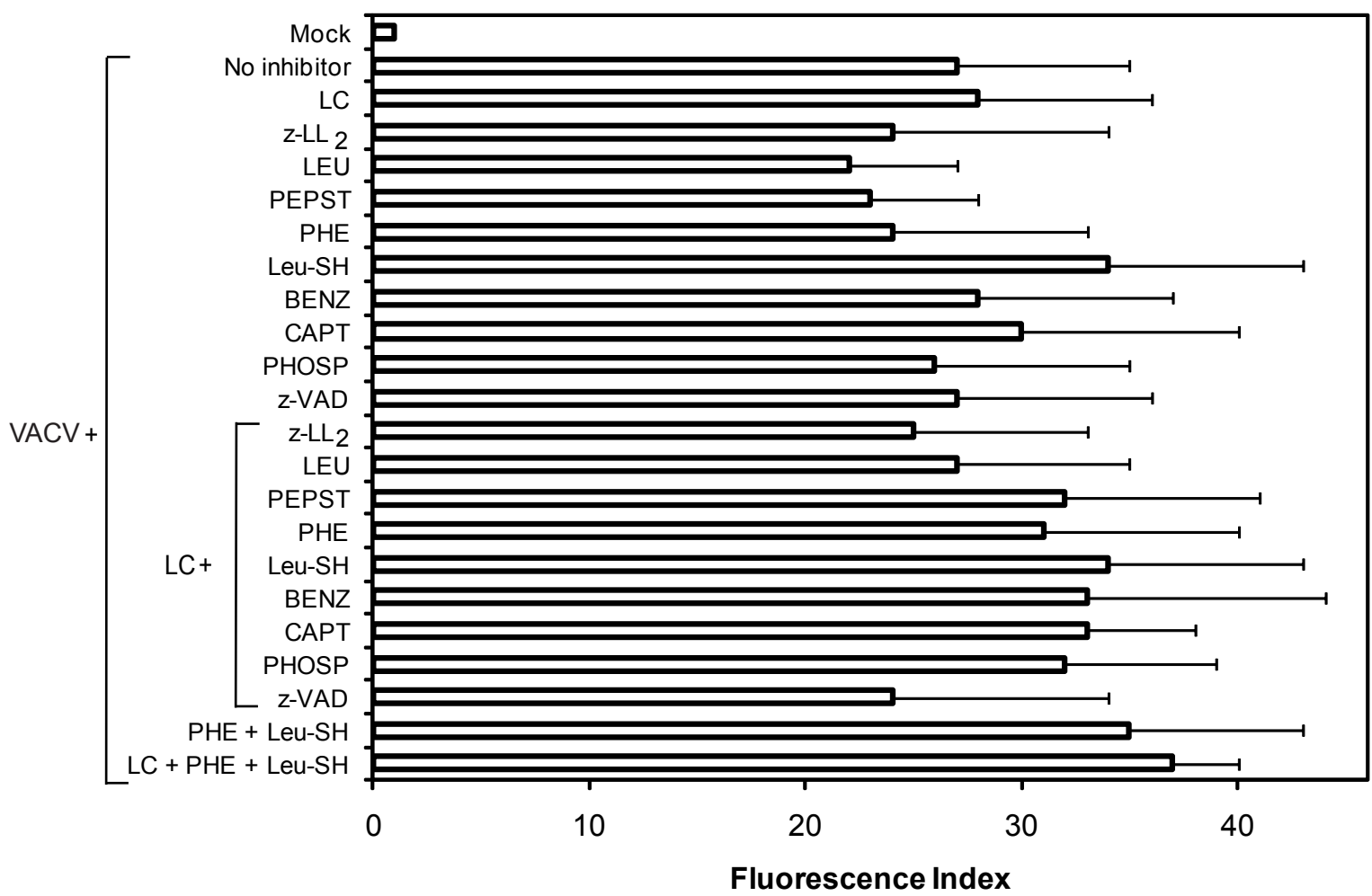
44

45 **Figure S5. Identification of three HLA ligands in infected cell extracts by mass**
46 **spectrometry (II).**

47

48 MS/MS fragmentation spectra obtained from quadrupole ion trap mass spectrometry of
49 the ion peaks at m/z 843.5 (upper left panel), m/z 833.9 (medium left panel), and m/z
50 851.0 (lower left panel) from the VACV-infected cell extract and the corresponding
51 synthetic peptide (right panels). The axes are as described in Figure S1.

52

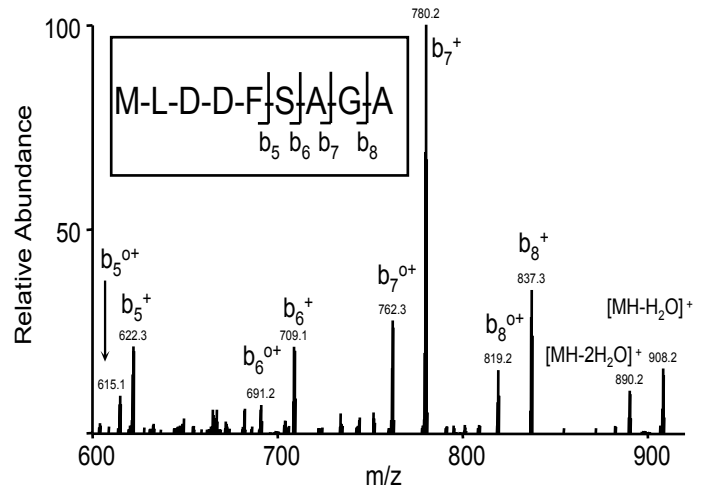
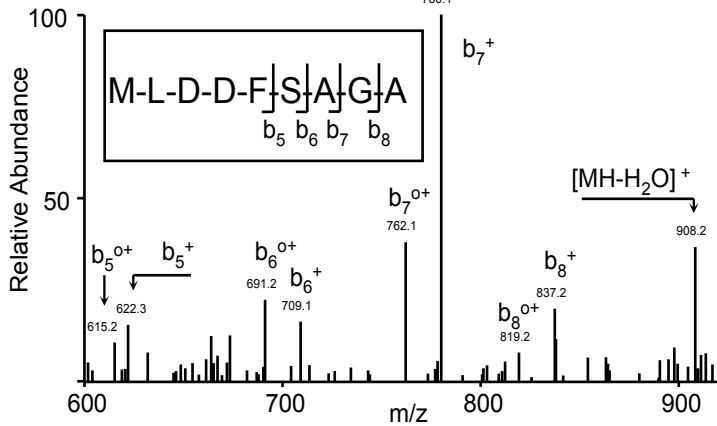


Lorente et al. Figure S1

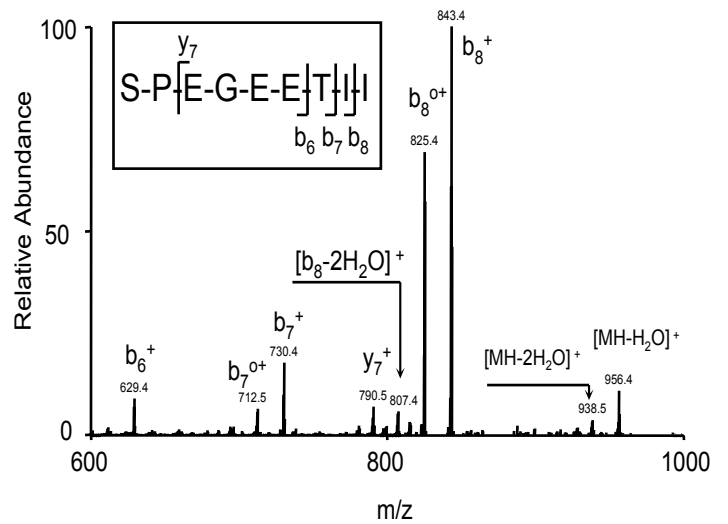
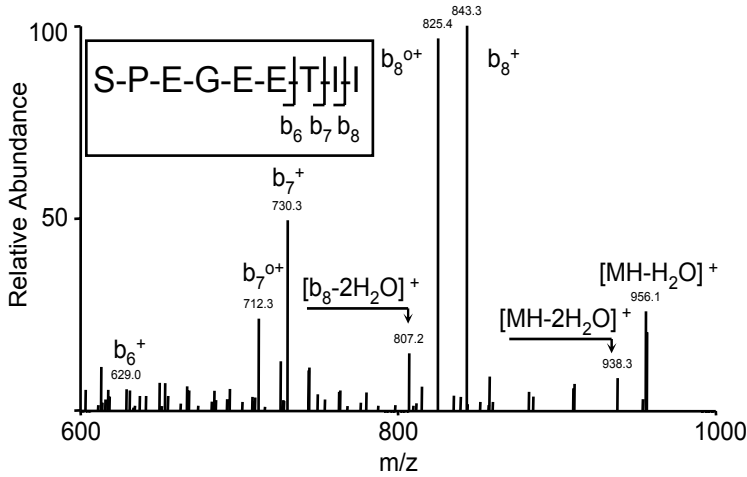
experimentally detected

synthetic

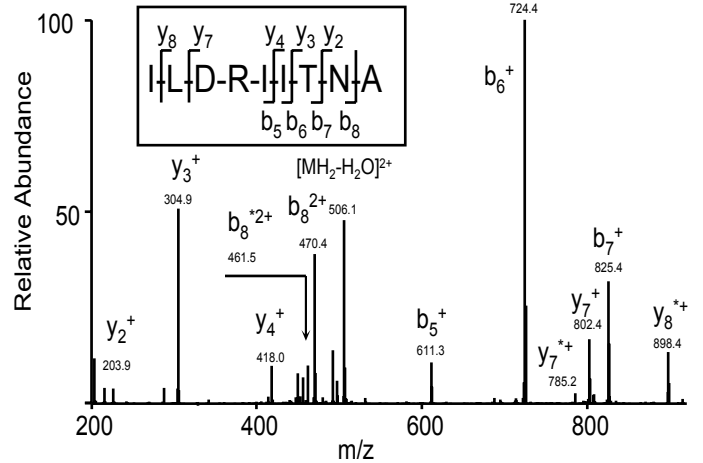
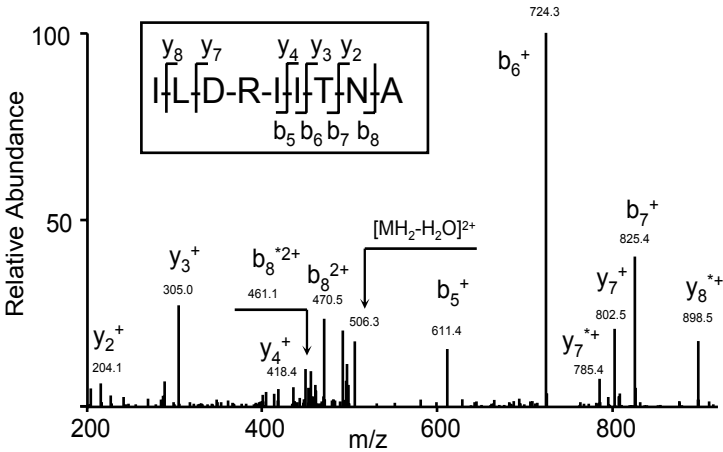
molecular ion at m/z 926.4



molecular ion at m/z 974.5



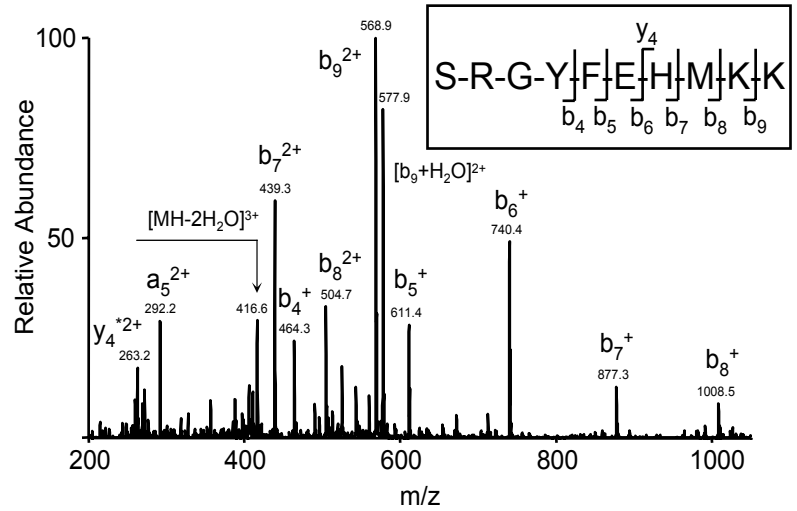
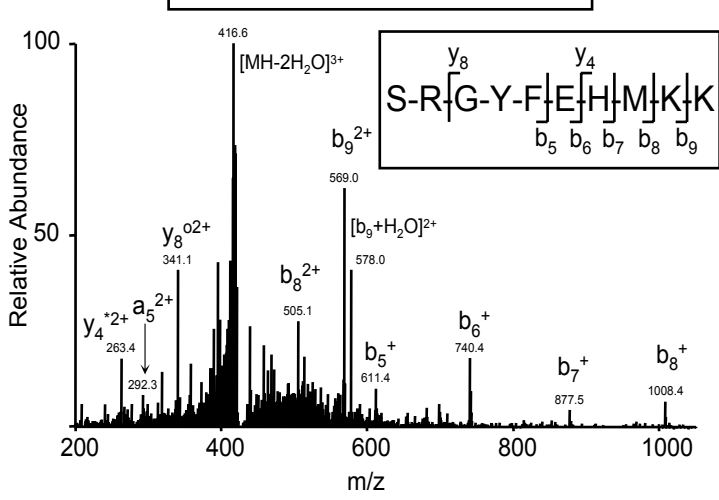
molecular ion at m/z 514.8



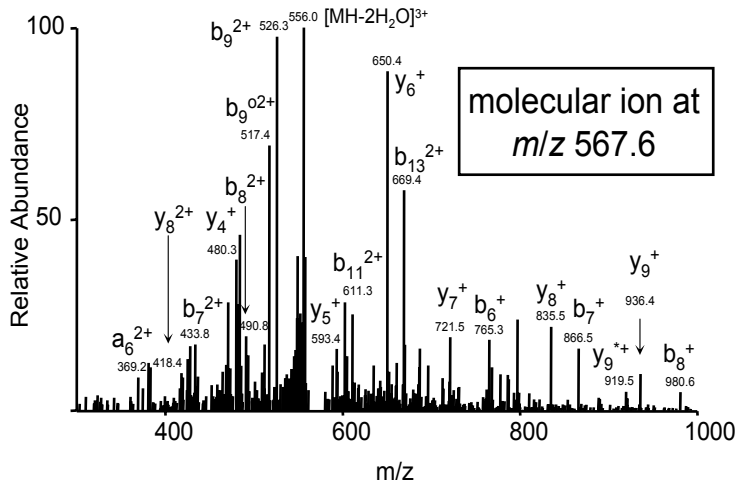
experimentally detected

synthetic

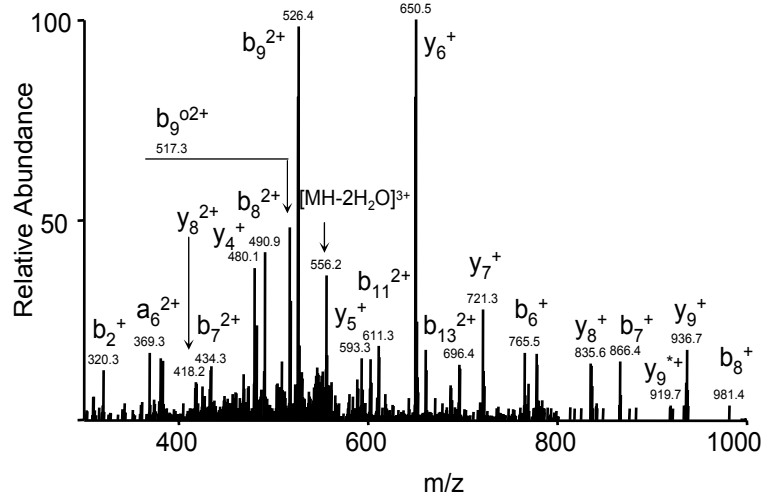
molecular ion at m/z 428.2



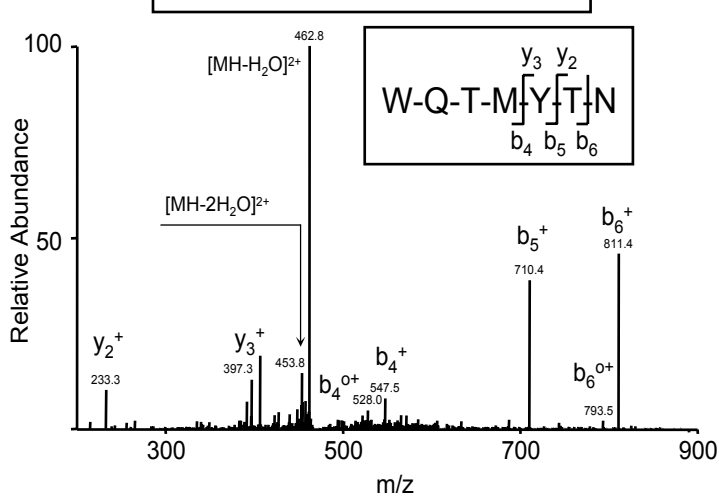
Y-R-L-Q-G-F-T-N-A-G-I-V-A-Y-K
 b_6 b_7 b_8 b_9 b_{11} b_{13}



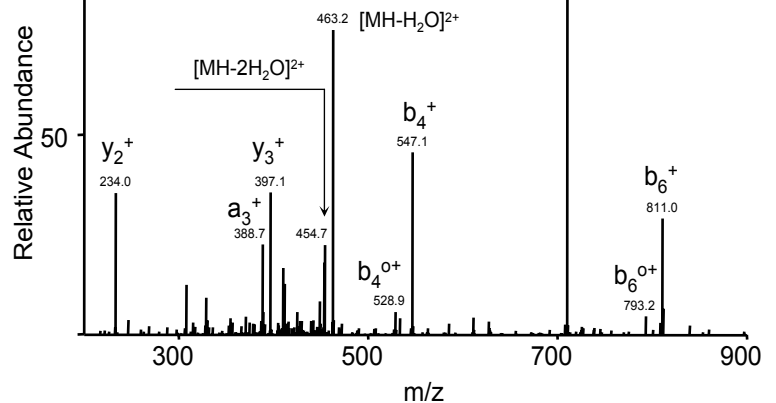
Y-R-L-Q-G-F-T-N-A-G-I-V-A-Y-K
 b_2 b_6 b_7 b_8 b_9 b_{11} b_{13}



molecular ion at m/z 472.1



W-Q-T-M-Y-T-N
 b_4 b_5 b_6



experimentally detected

synthetic

